Geological Quarterly, 2025, 69, 28
DOI: https://doi.org/10.7306/gq.1801

The impact of diagenesis on the reservoir properties of Mesozoic sedimentary rocks of the Łódź and Miechów troughs, central Poland

Aleksandra KOZŁOWSKA[1, *], Marta KUBERSKA[1], Anna FELDMAN-OLSZEWSKA[1], Anna MALISZEWSKA[1], Małgorzata POŁOŃSKA[1] and Krystyna WOŁKOWICZ[1]

[1] Polish Geological Institute-National Research Institute, Rakowiecka 4, 00-975 Warszawa, Poland; ORCID: 0000-0002-6360-4974 [A.K.], 0000-0002-3077-5718 [M.K.], 0000-0001-8870-5707 [A.F.-O.], 0000-0001-6902-5183 [K.W.]

Kozłowska, A., Kuberska, M., Feldman-Olszewska, A., Maliszewska, A., Połońska, M., Wołkowicz, K., 2025. The impact of diagenesis on the reservoir properties of Mesozoic sedimentary rocks of the Łódź and Miechów troughs, central Poland. Geological Quarterly, 69, 28; https://doi.org/10.7306/gq.1801

Associate Editor: Joanna Rotnicka-Dłużewska

Mesozoic siliciclastic and carbonate strata, analysed in 28 boreholes located in the Łódź and Miechów troughs, Poland, comprise Triassic and Jurassic rocks accumulated under terrestrial and marine conditions, and Cretaceous deposits of marine origin. Siliciclastic rocks (sandstones, siltstones, mudstones and claystones, with subordinate conglomerates) are the main lithofacies in the Lower and Upper Triassic, Lower and Middle Jurassic, and in the Lower Cretaceous. Carbonate rocks dominate in the Middle Triassic and Upper Jurassic. The Upper Cretaceous succession is represented by siliceous-carbonate deposits. These sedimentary rocks were studied in terms of sedimentary basin analysis and in particular as regards their reservoir characteristics, with detailed petrographic and porosity studies of these rocks and special emphasis on the sandstones and limestones. The focus was on the effects of diagenetic processes and their influence on reservoir properties. The most important diagenetic processes that affected the reservoir properties of the rocks were compaction, cementation and dissolution, and also replacement in carbonate rocks. Compaction and cementation have reduced the porosity of the sandstones by an average of ~44% and 29%, respectively. The effects of dissolution, mainly of feldspar grains and bioclasts, contributed to the development of secondary porosity in the rocks. Replacement processes – dolomitization of limestones – also increased the porosity of the rocks. Sandstones with good reservoir properties (porosity >15%, permeability >100 mD) are found in the Lower Triassic (Buntsandstein), Lower Jurassic and Lower Cretaceous. Among the carbonates, the Middle Triassic (Muschelkalk) deposits show the best reservoir properties, but most of the porous (>10%) carbonate and carbonate-marly rocks are impermeable. The Miechów Trough, by comparison with the Łódź Trough, includes better reservoir properties.

Key words: diagenesis, reservoir properties, Mesozoic sedimentary rocks, Łódź and Miechów troughs.

INTRODUCTION

We describe in detail the petrographic characteristics of Mesozoic rocks occurring to the south-west of the Mid-Polish Swell, in the Łódź and Miechów troughs, using core material from 28 boreholes (Fig. 1 and Table 1), and building on earlier petrographic studies on Mesozoic deposits in the Polish Lowlands (Maliszewska, 1999; Kuberska et al., 2023). Petrographic analyses are provided of Triassic, Jurassic and Cretaceous rocks. In the Triassic succession, the Buntsandstein has been investigated by Kuberska (e.g., 1997, 1999; Kuberska et al., 2019, 2023), the Muschelkalk by Wołkowicz (e.g., 1999; Kuberska et al., 2023) and the Upper Triassic by Maliszewska (e.g., 1972). In the Jurassic succession, the Lower Jurassic was studied by Kozłowska (e.g., Kozłowska et al., 2010; Kozłowska and Kuberska, 2014), the Middle Jurassic by Maliszewska (e.g., 1998, 1999; Kozłowska et al., 2021) and the Upper Jurassic by Wołkowicz (e.g., Połońska and Wołkowicz, 2005). The Cretaceous deposits were studied by Połońska (e.g., 1999a, b, 2000, 2007, 2010; Połońska and Wołkowicz, 2005). Petrographic data have been previously described both in the context of the geological structure of the study area and with respect to sedimentary conditions (e.g., Feldman-Olszewska 1997a, b, 1998a, b, 2012a, b).

The area of Łódź and Miechów troughs has also been previously studied, with focus on the Upper Cretaceous stratigraphy and sedimentology (Jurkowska, 2016), mineralogy (Jurkowska and Świerczewska-Gładysz, 2022) and palaeontology (e.g., Świerczewska-Gładysz, 2016; Świerczewska-Gładysz and Jurkowska, 2023).

* Corresponding author, e-mail: aleksandra.kozlowska@pgi.gov.pl

Received: March 21, 2024; accepted: July 3, 2025; first published online: September 9, 2025

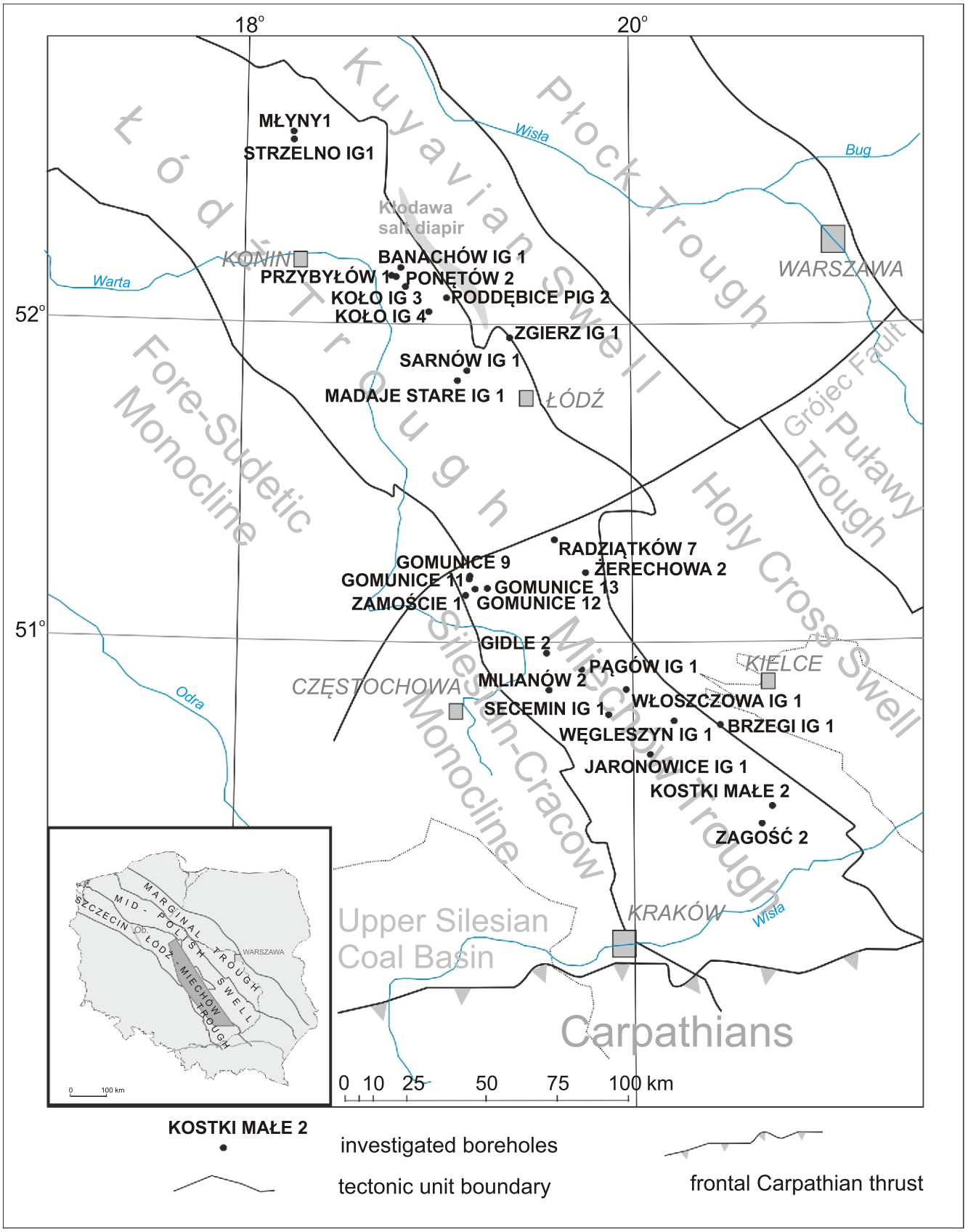

Fig. 1. Location map of the boreholes investigated in their tectonic context (after Stupnicka, 1989 and Narkiewicz and Dadlez, 2008; modified)

Ob. – Oborniki elevation

Table 1

Study data summary for stratigraphic units in the Łódź and Miechów troughs

Stratigraphy		Trough	Borehole	Rock type	Main lithofacies	Main diagenetic processes	Porosity (%)
Triassic	Lower (Buntsandstein)	Łódź	Zgierz IG 1	sandstones, siltstones mudstones, claystones	sandstones	compaction; cementation: carbonates („pure" calcite, Mn-calcite, dolomite, ankerite), quartz overgrowths on quartz grains, clay minerals (vermiform kaolinite); chlorites; anhydrite; dissolution (feldspar)	–
		Miechów	Brzegi IG 1, Gidle 2, Gomunice 9, 12, 13, Kostki Małe 2, Milianów 2, Pągów IG 1, Secemin IG 1, Węgleszyn IG 1, Zagość 2, Zamoście 1, Żerechowa 2.	sandstones, siltstones mudstones, claystones			0–19%
	Middle (Muschelkalk)	Łódź	Przybyłów 1, Zgierz IG 1.	limestones, mudstones	limestones	compaction; cementation: carbonates (calcite, dolomite), anhydrite, gypsum, quartz; dissolution (aragonite and calcite grains)	–
		Miechów	Brzegi IG 1, Gidle 2, Gomunice 9, 13, Jaronowice IG 1, Kostki Małe 2, Milianów 2, Pągów IG 1, Radziątków 7, Secemin IG 1, Węgleszyn IG 1, Włoszczowa IG 1, Żerechowa 2.	limestones, anhydrites			0–26%
	Upper (Keuper)	Łódź	Koło IG 4, Madje Stare IG 1, Poddębice PIG 2, Przybyłów 1, Strzelno IG 1.	sandstones, siltstones, mudstones, claystones, conglomerates, carbonates	sandstones	compaction; cementation: carbonates (calcite, dolomite, ankerite, siderite), quartz overgrowths on quartz grains, clay minerals (vermiform kaolinite); anhydrite; dissolution (feldspar); replacement	~1%
		Miechów	Gidle 2, 4, Gomunice 9, 11, 12, 13, Radziątków 7, Secemin IG 1, Węgleszyn IG 1, Żerechowa 2.	sandstones, claystones, mudstones, siltstones, carbonates			1–12%
Jurassic	Lower	Łódź	Banachów IG 1, Koło IG 4, Madaje Stare IG 1, Poddębice PIG 2, Ponętów 2, Zgierz IG 1.	sandstones, siltstones, mudstones, claystones, conglomerates	sandstones	compaction; cementation: quartz overgrowths on quartz grains, carbonates (siderite, ankerite, calcite), clay minerals (vermiform kaolinite, fibrous illite), chlorites; dissolution (feldspar)	7–16%
		Miechów	Gomunice 13, Pągów IG 1, Secemin IG 1, Węgleszyn IG 1, Włoszczowa IG 1.	sandstones, siltstones mudstones, claystones,			10–27%
	Middle	Łódź	Banachów IG 1, Koło IG 4, Madaje Stare IG 1, Poddębice PIG 2, Ponętów 2, Strzelno IG 1.	sandstones, siltstones, mudstones, claystones, conglomerates, carbonates	sandstones	compaction; cementation: carbonates (calcite, dolomite), quartz overgrowths on quartz grains,clay minerals (vermiform kaolinite, fibrous illite), chlorites, berthierine, anhydrite; dissolution (feldspar, carbonates)	–
		Miechów	Kostki Małe 2, Pągów IG 1, Secemin IG 1, Węgleszyn IG 1, Zagość 2, Żerechowa 2.	sandstones, claystones, mudstones, siltstones, carbonates			2–8%
	Upper	Łódź	Poddębice PIG 2, Ponętów 2, Przybyłów 1.	limestones, siltstones, mudstones, claystones, conglomerates	limestones	compaction; cementation: carbonates (calcite, dolomite, siderite), anhydrite, chalcedony; replacement (dolomitization, silicification); dissolution (carbonates)	–
		Miechów	Jaronowice IG 1, Kostki Małe 2, Milianów 2, Pągów IG 1, Secemin IG 1, Węgleszyn IG 1, Włoszczowa IG 1, Zagość 2, Żerechowa 2.	limestones, claystones, mudstones, siltstones			1–14%

Tabl. 1 cont.

Cretaceous	Lower	Łódź	Banachów IG 1, Koło IG 4, Madaje Stare IG 1, Poddębice PIG 2, Ponętów 2, Sarnów IG 1, Strzelno IG 1	limestones, anhydrites, claystones, mudstones, siltstones, sandstones, conglomerates	sandstones, limestones	compaction; cementation: quartz overgrowths on quartz grains, carbonates (calcite, siderite), clay minerals (vermiform and blocky kaolinite); chlorite rims; dissolution (feldspar, calcite) compaction; cementation: carbonates (calcite, dolomite, ankerite), clay minerals (kaolinite); dissolution (bioclasts)	15–28% 2–4%
		Miechów	–				–
	Upper	Łódź	Banachów IG 1, Koło IG 4, Młyny 1 Poddębice PIG 2, Sarnów IG 1, Strzelno IG 1	limestones, opokas, sandstones, claystones, mudstones, siltstones	sandstones, limestones	cementation: quartz overgrowths on quartz grains, chalcedony, carbonates (calcite, siderite), clay minerals (vermiform and blocky kaolinite), chlorites; compaction; dissolution (feldspar) cementation: carbonates (calcite, dolomite, ankerite), clay minerals (kaolinite), opal; compaction	3%
		Miechów	Pągów IG 1	limestones, opokas, sandstones, conglomerates, claystones, mudstones, siltstones			3%

The lithological and diagnetic characteristics of the rocks in question are important factors in considering the development within them of pore space and reservoir properties. Karnkowski (1993) noted evidence of hydrocarbon-generating processes in the Łódź Trough from oil and gas shows in the Koło IG 3, Koło IG 4, Ponętów 1 and Przybyłów 1 boreholes. This recognition has prompted our analysis of this succession, particularly the sandstones and limestones, to determine the influence of diagenesis on the petrophysical properties of the rocks as regards exploration for hydrocarbon accumulations in the Polish Lowlands. Detailed petrographic and porosity studies of these rocks were undertaken and combined with the results of previous studies, to determine which of the Mesozoic units studied have the best reservoir properties, and which of the two areas of study are the most prospective for hydrocarbon exploration.

GEOLOGICAL SETTING, LITHOLOGY AND SEDIMENTARY ENVIRONMENTS

The Łódź Trough covers the central part, and the Miechów Trough the south-eastern part, of the Szczecin-Łódź-Miechów Trough (Fig. 1; Stupnicka, 1989; Narkiewicz and Dadlez, 2008). The troughs are located on the SW side of the Mid-Polish Swell, the NW-SE trend of which is closely related to the strike of the Teysseyre-Tornquist Zone. Evolution of the troughs is related to tectonic inversion of the axial part of the sedimentary basin, i.e. the Mid-Polish Trough, which resulted in the formation of the Mid-Polish Swell. Filled with Permian-Mesozoic strata, the Mid-Polish Trough was uplifted and strongly eroded at the Cretaceous/Paleogene transition (Late Turonian?/Coniacian-Paleocene; Krzywiec, 2006; Krzywiec et al., 2009). On both sides of the emerging Mid-Polish Swell, the Marginal Trough and the Szczecin-Łódź-Miechów Trough were formed, the boundaries of which are marked by the present-day limit of Cretaceous deposits (Stupnicka, 1989).

The north-eastern boundary of the Łódź Trough is partly tectonic in nature and runs along the Kłodawa salt diapir, which is separated from the Łódź Trough by NW–SE-trending fault zones (Dadlez, 1998). The western boundary of the Łódź Trough (with the Szczecin Trough) runs along the western edge of the Oborniki Elevation (Pożaryski, 1969; Marek, 1977a; Dadlez, 1997), whereas its south-eastern boundary with the Miechów Trough is drawn at an extension of the Grójec Fault (Pożaryski, 1969; Narkiewicz and Dadlez, 2008; Złonkiewicz, 2006, 2009). The basement of the Łódź Trough is probably represented by folded rocks of the Variscan Orogen, whereas the Miechów Trough is located mostly on the Małopolska Block (Narkiewicz and Dadlez, 2008; Buła and Habryn, 2010). The southern part of the Miechów Trough is overlain by Cenozoic deposits of the Carpathian Foredeep. Farther south, it dips beneath the Carpathian Overthrust.

Both the Łódź Trough and the Miechów Trough are filled with Permian-Mesozoic deposits, but they differ in terms of the thickness of the individual stratigraphic units and their age range (Fig. 2). They also differ with regard to the presence or absence of manifestations of salt tectonics. The Łódź Trough area is located in the marginal zone of an area of salt pillows and diapirs (Dadlez, 1998) composed of Zechstein deposits, active in Late Triassic, Early and Middle Jurassic, and Late Cretaceous times. Numerous salt pillows and a salt diapir occur in this area (Marek, 1977a). No signs of salt tectonic activity are found in the Miechów Trough area.

Detailed information on the lithology and sedimentary environments of Mesozoic formations in the Łódź and Miechów troughs are given in Figure 2.

The Triassic section in the Łódź Trough has no stratigraphic gaps and begins with Buntsandstein strata (Szyperko-Śliwczyńska, 1977; Gajewska, 1977; Dadlez and Franczyk, 1977). These are represented by red fine-grained siliciclastic deposits with interbeds and lenses of marly limestone (Szyperko-Śliwczyńska, 1979, 1980; Szyperko-Teller, 1997). In the Miechów Trough, the Lower and Middle Buntsandstein occur only in its northern and central parts (Jurkiewicz, 1973). The lowermost part is lithologically the same as in the Łódź Trough, while higher in the section there are mainly red sandstones (an informal "Sandstone" formation) (Szyperko-Teller, 1997; Fijałkowska-Mader et al., 2015). The Middle Buntsandstein sedimentary basin became more uniform lithologically. In the Łódź and Miechów troughs, the lower part of the section is repre-

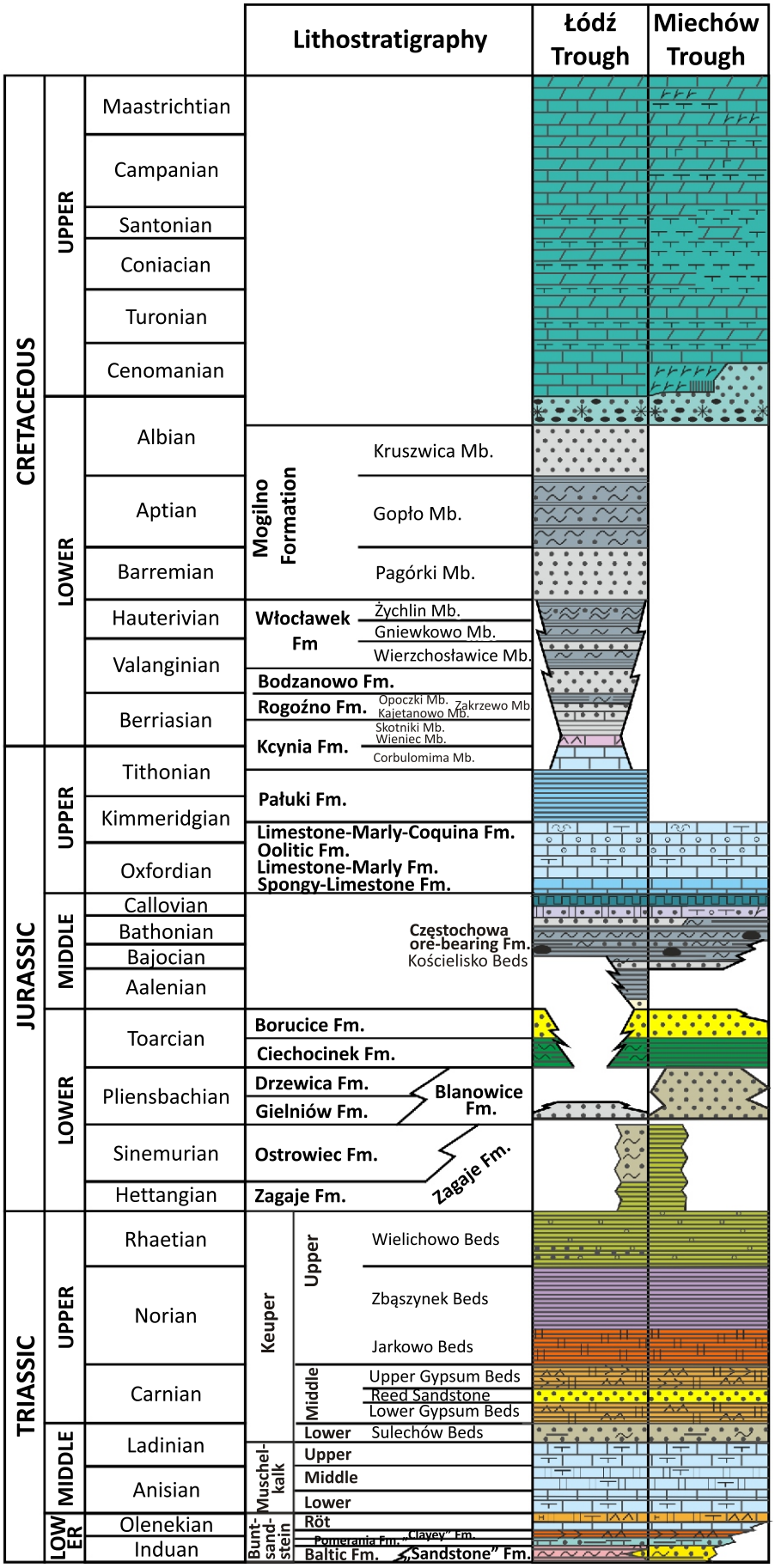

Fig. 2. Lithology and sedimentary environments of Mesozoic lithostratigraphic units in the Łódź Trough and Miechów Trough after: Jurkiewicz (1973), Mrozek (1975), Gajewska (1977, 1978, 1988a, 1997), Marek (1977b, 1997), Szyperko-Śliwczyńska (1977, 1980), Błaszkiewicz and Cieśliński (1979), Dembowska (1979), Kopik (1979), Marek and Raczyńska (1979), Senkowiczowa (1979), Szyperko-Teller (1982, 1997), Deczkowski (1997), Krassowska (1997), Niemczycka (1997), Feldman-Olszewska (1998a, b), Pieńkowski (2004), Złonkiewicz (2009), Fijałkowska-Mader et al. (2015)

Fm. – Formation, Mb. – Member

Fig. 2. cont. Legend

sented by sandstones of the Pomerania Formation, while the upper part is composed of claystones (an informal "Clayey" formation) (Szyperko-Śliwczyńska, 1977; Szyperko-Teller, 1982, 1997; Fijałkowska-Mader et al., 2015). Deposition of the Upper Buntsandstein occurred throughout both basins (Szyperko-Teller, 1997). It was characterized by cyclic stages of stagnation combined with increased evaporation and renewed transgressions. In both troughs, the section is composed of carbonate rocks with intercalations of gypsum, anhydrite and salts (Röt lithofacies) (Jurkiewicz, 1973; Szyperko-Teller and Moryc, 1988; Szyperko-Teller, 1997).

This type of lithology passes continuously into Middle Triassic limestones of the Muschelkalk unit (Senkowiczowa, 1979; Gajewska, 1988a). Deposition took place in an epicontinental marine basin, periodically of elevated salinity. During sedimentation of the Lower Muschelkalk, the marine transgression reached its peak (Narkiewicz and Szulc, 2004). The Middle Muschelkalk marks a change in lithofacies that resulted in the deposition of calcareous-marly sediments throughout almost the entire basin. The uppermost part of the Middle Triassic is composed mostly of sandstones (Lower Keuper deposits) (Gajewska, 1978).

Upper Triassic deposits in the Łódź and Miechów troughs are represented by siliciclastic rocks, predominantly claystones of red, green and variegated colours with intercalations of anhydrite, gypsum, dolomite and sphaerosiderite, deposited in a hot, mostly dry climate (Gajewska, 1988b, Deczkowski, 1997, Fijałkowska et al., 2015).

The Lower Jurassic section is significantly reduced in the Łódź Trough in terms of both the thickness and the range of its stratigraphic units. This area was a positive element in relation to adjacent areas at that time (Dadlez and Franczyk, 1976). In

its central part there are only sandstones of presumed Pliensbachian age. In more peripheral zones, Toarcian deposits also successively appear (Dadlez and Franczyk, 1977; Feldman-Olszewska, 2012a). Over most of the Łódź Trough area, Aalenian and Lower Bajocian strata are absent, and the Upper Bajocian section is reduced. These deposits occur only at the boundary with the Kuyavian Swell, in a graben of increased subsidence rate (Feldman-Olszewska, 2012b), and in the eastern part of the Łódź Trough (Dayczak-Calikowska, 1977). The Bathonian section is dominated by marine fine-grained siliciclastic deposits, while the Callovian succession is represented by carbonate-siliciclastic rocks.

In the Miechów Trough, Lower Jurassic deposits occur only in the northern and central parts (to the Secemin IG 1–Włoszczowa IG 1 line in the south). In this area, a geological section similar to that in the marginal zone of the Łódź Trough is observed, with mainly Pliensbachian deposits overlain by Toarcian rocks (Mrozek, 1975). In addition, the Hettangian-Sinemurian deposits, reduced in thickness, occur only at the boundary with the Łódź Trough. The Middle Jurassic section, as in the Łódź Trough, is composed of Bajocian and Bathonian siliciclastic rocks and Callovian carbonate-siliciclastic deposits with a condensed bed of a starved shelf in its uppermost part (Dayczak-Calikowska and Moryc, 1988; Feldman-Olszewska, 1997b, 1998b; Złonkiewicz, 2009). Towards the south, the Middle Jurassic deposits are increasingly reduced and wedged out.

In the Late Jurassic, the subsidence axis ran across the NE part of the Łódź Trough. This area shows a complete Upper Jurassic section encompassing several carbonate and marly-clayey formations (Dembowska, 1979). In the NE zone of the Łódź Trough, there is a continuous Jurassic to Cretaceous transition (Dembowska, 1977). In the Miechów Trough area, only Oxfordian and Lower Kimmeridgian carbonates have been preserved, which can be correlated with the formations distinguished in the Łódź Trough area (Dembowska, 1979; Niemczycka, 1997; Złonkiewicz, 2009).

A fully developed Lower Cretaceous section (Berriasian-Albian) in the Łódź Trough is found only in the NE zone (Marek, 1977b). To the south-west of the zone, the Lower Cretaceous section starts with the Upper Valanginian or Hauterivian. The absence of the lower Lower Cretaceous in this area is related to the presence of a positive, rigid element in the basement (active also during the Early and Middle Jurassic). Farther to the south-east, the Lower Cretaceous deposits wedge out and only Albian rocks are present in the Miechów Trough (Hakenberg et al., 1973; Hakenberg, 1986).

Upper Cretaceous deposits are found over the whole area of the Łódź and Miechów troughs. Throughout the entire Łódź Trough, there are Cenomanian to Campanian deposits, and the Maastrichtian is found in its central part (Jaskowiak-Schoeneichowa and Krassowska, 1988; Leszczyński, 2010). The Cretaceous succession of the Miechów Trough is represented by Cenomanian to Maastrichtian strata (Błaszkiewicz and Cieśliński, 1979). The Upper Cretaceous rocks form a single evolutionary cycle of a marine sedimentary basin with pelagic carbonate and carbonate-siliciclastic deposition (Krassowska, 1997). Moreover, in the vicinity of the salt diapirs, siliciclastic-carbonate successions composed of sandstones, opokas and marls, locally also with mudstone interbeds, are observed (Leszczyński 2000, 2010). These are interpreted as submarine fans of gravity flows generated by upward movements of Permian salt masses.

ANALYTICAL METHODS

The material for this study comes from 28 boreholes drilled in the Łódź and Miechów troughs (Fig. 1). About 430 rock samples were taken, ~150 from Triassic, ~160 from Jurassic and ~120 from Cretaceous rocks. They were roughly equally divided between sandstones and carbonate rocks, and used to produce thin sections. Prior to thin section preparation, some core samples (mainly sandstones) were saturated with blue-coloured resin for subsequent pore space observation. Computer image analysis was performed on 34 such sections to define their pore space and to determine their porosity level using NIS-Elements software. The resolution of the images taken for computer analysis was 5 millions pixels. The porosity was also measured during planimetric analyses by counting 300 points per thin section using a polarizing microscope. The mineral composition of the rocks, their structures and textures, as well as the progress of mechanical and chemical compaction and the effects of other diagenetic processes (cementation, dissolution, replacement, alteration and neomorphism), were determined by thin section analysis. Most sections were stained with Evamy's solution for the preliminary identification of the chemical composition of carbonates (Migaszewski and Narkiewicz, 1983). The study was also aided by cathodoluminescence (CL) analysis performed on approximately 80 thin sections, using a CCL 8200 mk 3 instrument from Cambridge Image Technology Ltd, mounted on a Nikon Optiphot 2 polarizing microscope table. In many cases, the analysis enabled distinction between different generations of cements, allowed recognition of the outlines of mineral grains and bioclasts that had been obliterated, for example, by silicification processes or impregnation with iron compounds, and identification of the zonal structure of some crystals.

Results of scanning electron microscope (SEM) studies of the rocks, using *JEOL JSM-35* and *LEO 1430* instruments connected with an *EDS ISIS* energy dispersive spectrometer, were also used. 51 rock samples and ten thin sections were examined. The microlithofacies varieties of rocks were determined using the classification of sandstones by Pettijohn et al. (1972), modified by Jaworowski (1987) and Ryka and Maliszewska (1991), and the Folk (1959) and Dunham (1962) classifications and their modifications for carbonates.

Investigations of fluid inclusions in cements were performed on four sandstone samples in special doubly polished plates. Fluid Inc. System equipment (manufactured in the USA) mounted on a Leitz – Orthoplan polarizing microscope, and a THMS600 heating and freezing table from Linkam Scientific Instruments Ltd. installed on a *Nikon Eclipse LV100 POL* polarizing microscope, were used. The heating and freezing of samples on freezing and heating stages were carried out at temperatures ranging from room temperature (23°C) to +120°C and to –80°C (occasionally to –120°C). The measuring accuracy for both stages was calibrated against SynFlinc standards. *FLUIDS* software (Bakker, 2003) was used to calculate salinity. Inclusion associations were interpreted based on the proposal by Goldstein and Reynolds (1994).

X-ray studies were carried out on a *Philips PW 3020* X-ray diffractometer equipped with an *APO 1877* automated computer identification system. Five mudstone samples and one sandstone and one limestone sample were analysed in oriented air-dried preparations, after glycolation and heating.

Porosimetric studies and permeability determinations on 56 selected rock samples, mainly sandstones, were carried out at the Oil and Gas Institute in Kraków. The following were determined: the total porosity coefficient (expressing the ratio of the volume of all pores (open and closed) to the total volume of the rock sample studied); the effective porosity coefficient (expressing the ratio of the volume of open connected pores to the total volume of the rock sample studied); and the dynamic porosity coefficient (expressing the ratio of the volume of pores from which formation fluids can be recovered to the total volume of the sample studied). The total porosity coefficient was determined using the pycnometric method, and the effective porosity coefficient was calculated by saturating the sample with a wetting liquid. Knowing the density of the liquid used for the test, the volume of open pores was calculated. Parameterization of the pore space was obtained by measuring capillary pressure curves. This study used the dependence of capillary pressure magnitude on the radius length, its shape, and the network of interconnections between pores of different radii. The capillary pressure curves were obtained using the porosimetric method, i.e. a method of injecting mercury into test samples. An *AutoPore9220* mercury porosimeter was used. The effective permeability coefficient was determined using nitrogen.

RESULTS

LITHOFACIES AND MINERAL COMPOSITION

The deposits analysed in this study are dominated by siliciclastic and carbonate lithofacies. Siliciclastic rocks are represented by claystones, mudstones, siltstones, sandstones and occasional conglomerates. Carbonate rocks comprise limestones and dolomites, and their marly varieties – marls, or silicic varieties – opokas (carbonate-siliceous rocks that contain silica polymorphs in the form of opal-CT and small amount <10% of detrital quartz and clay) and gaizes (rocks which contain higher >10% content of detrital quartz compared to opokas) (Jurkowska and Świerczewska-Gładysz, 2022; Table 1).

TRIASSIC (FIG. 3)

Conglomerates are a subordinate lithofacies in the Triassic section. In the Middle Triassic, intraformational calcareous conglomerates are found at the boundary between the Łódź Trough and the Miechów Trough. In the Upper Triassic, conglomerates composed mainly of dolomite clasts are reported. Conglomerates are the most common lithofacies in the Norian. These are red finely bedded clay conglomerates composed mainly of Keuper claystones cemented by clay (Koło IG 4, Strzelno IG 1), as well as finely bedded polymictic conglomerates, conventionally referred to as the "Lisów Breccia" (Maliszewska, 1972). The groundmass in these rocks is composed of quartz, feldspar and mica grains, as well as of clay and carbonate minerals and iron hydroxides.

Sandstones (Fig. 3A–D) are a significant lithofacies in the Lower and Upper Triassic. They represent very fine-grained and fine-grained varieties. Medium-grained sandstones are more abundant in the southern part of the study area, where coarse-grained, conglomeratic varieties may also be found. In view of the mineral composition of the detrital material and the proportion of clayey-muddy matrix, the Lower Triassic sandstones are classified as arenites and wackes, quartz and subarkosic, less frequently sublithic, in contrast to the Upper Triassic sandstones dominated by sublithic varieties (Fig. 4). The degree of sorting of detrital material in the fine-grained sandstones is good; coarser-grained varieties are characterized by poorer sorting. The grain point contacts ratio usually does not exceed 2.5. Straight and point contacts are most frequent; less frequent are concavo-convex ones. The main component of all sandstones is mono- and polycrystalline quartz. In arkosic varieties, feldspars are an important constituent. Among the lithoclasts, fragments of sedimentary rocks, as well as clasts of effusive and metamorphic rocks, definitely dominate. These are more common in sublithic varieties of the sandstones.

In addition, muscovite and biotite flakes (Fig. 3A) and calcite ooids are common in the Lower Triassic (Kuberska, 1997, 1999). Carbonaceous plant remains and dispersed organic matter are found in the Upper Triassic. The grain framework and matrix are cemented by carbonates, quartz, authigenic clay minerals and anhydrite. The matrix consists of muddy-clayey ferruginous matter and is present in almost all sandstone types. Carbonates are common in the cements; calcite is more frequent than dolomite, and ankerite is locally present. An additional component of the Upper Triassic sandstones is siderite. Cathodoluminescence analysis has enabled identification of two varieties of calcite: non-luminescent, so-called pure calcite, and Mn-calcite, showing yellow luminescence (Fig. 3B). Pure calcite, previously reported in the Kuyavian region (Kuberska, 1999), does not show any admixtures of other chemical elements. It was found only in Lower Triassic sandstones. The other calcite variety is characterized by the presence of Mn^{2+} activator ions in the crystal lattice (Sikorska, 1994). Locally, this calcite contains admixtures of iron, as shown by yellow-red luminescence or a blue-violet coloration of the carbonate after treatment of the thin section with Evamy's solution. Investigations of fluid inclusions in calcite (Lower Triassic) indicate the presence of primary and secondary, two-phase and single-phase inclusions. The homogenization temperatures are not highly variable and range from 90 to 120°C. The results of measurements of ice melting temperatures of the inclusions studied indicate that the fluids in the individual samples are complex, and difficult to express in terms of NaCl equivalent values. The eutectic temperatures close to (–60)°C suggest the inclusions contain brine systems that are more complex than the NaCl-H_2O system, such as H_2O-NaCl-$CaCl_2$-$MgCl_2$ (Bodnar, 1990). Dolomite occurs as either subhedral crystals filling pore spaces or as rhombohedra, commonly showing a zonal structure. Ankerite is rare and mostly forms the margins of Fe-dolomite grains. Authigenic quartz (1–22 vol.% of rock) is also present, creating overgrowths on detrital grains or filling pore spaces (Fig. 3C). Aggregates of authigenic clay minerals, kaolinite (Fig. 3D), chlorite, and subordinate illite, have also been identified. Authigenic feldspar overgrowths are not frequent (up to 1 vol.% of rock). In the cements, anhydrite is more common in rocks from boreholes located in the Łódź Trough (Kuberska, 1999) and in the northern part of the Miechów Trough.

Mudstones and siltstones (Fig. 3E) are common in both the Lower Triassic (thick brownish-red or greyish-green packets in the top parts, or interbeds in sandstones and claystones) and the Upper Triassic (most abundant in the Lower and Upper Gypsum Beds – Keuper; they have also been reported from the Reed Sandstone). They are represented mostly by quartz siltstones. In addition to the commonly present quartz and feldspars, enrichment in micas, mainly muscovite and biotite, is a characteristic feature. These grains are cemented by detrital clay minerals and authigenic components: kaolinite, quartz, calcite, Fe-dolomite, ankerite and siderite. The siltstones also contain iron hydroxides, pyrite, organic matter, coalified plant detritus, and locally anhydrite.

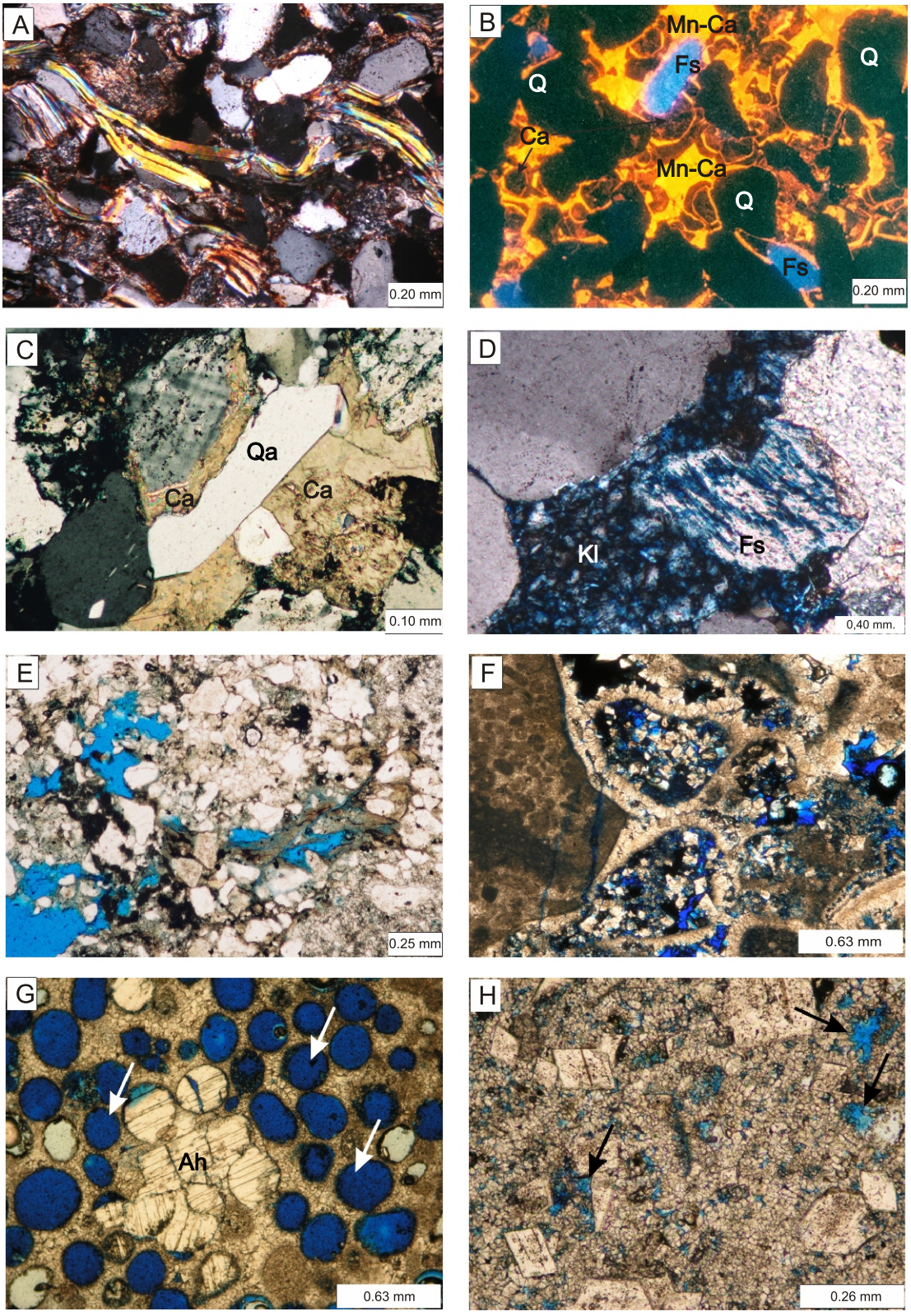

Fig. 3. Photomicrographs taken using a polarizing microscope (PL) and by cathodoluminescence (CL)

A – mica flakes bent as a result of mechnical compaction. Brzegi IG 1 borehole, depth 1496.2 m, Lower Triassic, PL, crossed polars; **B** – calcite cement in sublithic arenite; Mn-Ca – manganese-calcite, Ca – „pure" calcite, Fs – feldspar, Q – quartz. Gomunice 13 borehole, depth 2264.2 m, Lower Triassic, CL image; **C** – subarkosic arenite; authigenic quartz (Qa) surrounded by calcite (Ca). Gomunice 9 borehole, depth 1394.8 m, Upper Triassic, PL, crossed polars; **D** – subarkosic arenite; partly dissolved potassium feldspar (Fs) and kaolinite (Kl) in pore space of sandstone. Brzegi IG 1, depth 1529.3 m, Lower Triassic, sample impregnated by blue resin, PL, crossed polars; **E** – porous sandy siltstone. Secemin IG 1 borehole, depth 1411.2 m, Upper Triassic, sample impregnated by blue resin, PL, without analyzer; **F** – grainstone; dolomite rhombohedra in pore space (blue colour). Gidle 2 borehole, depth 1740.4 m, Middle Triassic, sample impregnated by blue resin, PL, without analyzer; **G** – grainstone; voids of dissolved grains (arrows) and anhydrite cement (Ah) are visible. Gidle 2 borehole, depth 1788.3 m, Middle Triassic, sample impregnated by blue resin, PL, without analyzer; **H** – dolomitized crystalline limestone with pores (arrows, blue colour). Secemin IG 1 borehole, depth 1888.3 m, Middle Triassic, sample impregnated by blue resin, PL, without analyzer

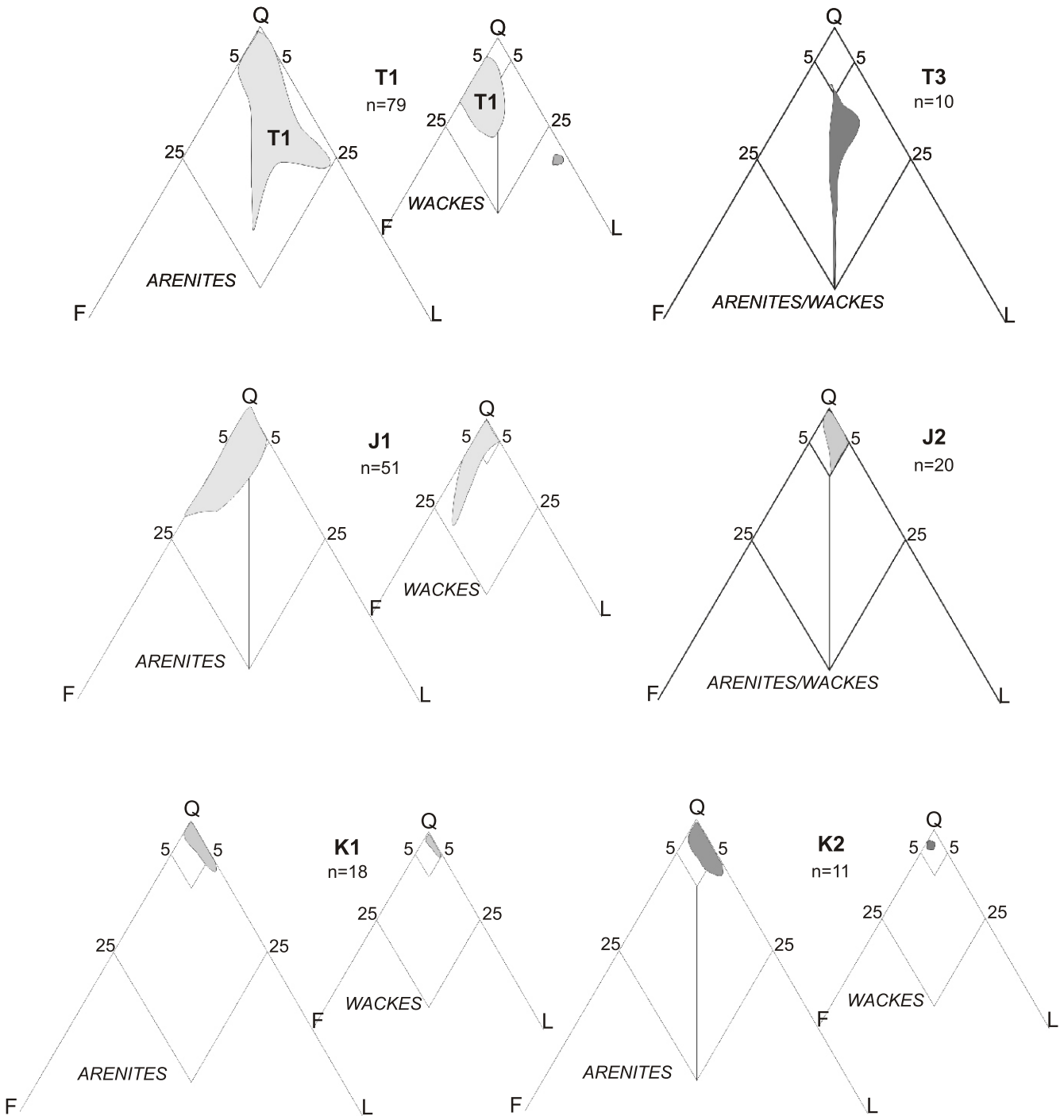

Fig. 4. Classification triangles of Pettijohn et al. (1972), modified by Jaworowski (1987) and Ryka and Maliszewska (1991), for the Triassic, Jurassic and Cretaceous sandstones

Q – quartz, F – feldspars, L – lithoclasts; T1 – Lower Triassic, T3 – Upper Triassic, J1 – Lower Jurassic, J2 – Middle Jurassic, K1 – Lower Cretaceous, K2 – Upper Cretaceous; n – number of analyses

The claystones are composed of clay-size detrital material with a minor admixture of silt and sand of quartz and feldspar, and mica flakes. The mineral compositions of the Lower, Middle and Upper Triassic claystones are similar. The Rhaetian claystones are locally interbedded with clayey siderites (Dadlez, 1973).

Carbonate rocks (Fig. 3F–H) are the main lithofacies in the Muschelkalk succession. They are also found, less frequently, in the Lower and Upper Triassic. Limestones are represented by microsparite and micrite varieties with prominent bioclasts, ooids and detrital material. These are micrite clayey-sandy limestones (mudstones and wackestones) and organodetrital limestones (packstones and grainstones). Other constituents include bivalve and gastropod remains, commonly pyritized, crinoid stems, and echinoderm plates. Allogenic material is represented by grains of quartz and occasionally of feldspar. Clay minerals and pyrite are also observed, and peloids and ooids showing varying degrees of preservation of internal structure.

The cements in the Muschelkalk rocks are composed predominantly of calcite, which is locally admixed with Mn and Fe. There are also dolomite, Fe-dolomite, anhydrite, gypsum, pyrite, sphalerite, barium celestine, halite, authigenic quartz, and feldspar with a composition similar to albite. In the Kuyavian area, carbonate cements in the Lower Muschelkalk have a calcite and Mg-calcite composition; dolomite is a minor component, being rarely admixed with Fe, or Mn and Fe. In the Upper Muschelkalk, an admixture of Mn (in addition to Fe and Mg) has been found in the calcite cements; dolomite and ankerite are also present (Wołkowicz, 1999).

The limestones, especially in the Upper Buntsandstein, reveal voids and fractures filled with anhydrite (Fig. 3G). There are also stylolites filled with clay-ferruginous matter with an admixture of organic matter. Dolomites (Fig. 3F, H) have been encountered, for instance in the Upper Buntsandstein and in the Keuper. These are micrite and microspar and spar rocks, which are largely sandy. They contain quartz and weathered feldspar grains, and clasts of quartz schist, siliceous rocks and micas, as well as organic matter. Individual calcite grains, presumably bioclasts, are also visible. Phosphate debris and anhydrite were noted. Dolomite-anhydrite lenses, intercalations and interbeds are present in places (Gidle 2, Gomunice 9, 11, Secemin IG 1, Węgleszyn IG 1). Intergranular spaces are filled with rhombohedral dolomite cement (Fig. 3F), blocky calcite cement, or siliceous cement.

In the Poddębice PIG 2 borehole (Keuper) there are grey dolomitic marls with fine quartz grains, iron hydroxides, plant detritus, and pyrite.

JURASSIC (FIG. 5)

Conglomerates are rare and occur only locally in the Jurassic strata. In the Lower Jurassic, a light grey polymictic/quartz rudite was found (Poddębice PIG 2, depth 3621.3 m). It contains ~60 vol.% of rounded gravel grains with a most common diameter of 3.0 mm and a maximum diameter of 15.0 mm. In addition to pale quartz grains (commonly as “vein” quartz), there are also clasts of grey and black claystone. The groundmass is composed of coarse-grained quartz arenite, and the cement is of authigenic quartz, kaolinite, illite flakes, and carbonaceous matter. In the Middle Jurassic section, conglomerates were found in the Bajocian of the Strzelno IG 1 borehole (Ryll, 1973). They form layers between finer-grained rocks, and their thickness varies from 10 to 145 cm, averaging ~30–40 cm. They are composed of ellipsoidal, well-rounded carbonate and siliciclastic rock clasts, ranging in diameter from 2 mm to 2 cm, cemented predominantly by siderite. The Upper and Middle Bathonian conglomerates (Madaje Stare IG 1 borehole) are largely finely bedded, with a most common gravel diameter of 0.5 cm (Maliszewska, 1971). Their main components are pebbles of siderite-cemented quartz sandstone containing numerous chamosite or berthierine ooids. Some of the ooids are sideritized. Bryozoan and serpulid fragments and bivalve shells occur in the sandstone clasts. Grains of quartz and clasts of chamosite or berthierine rocks have also been seen in the psephitic fraction of the conglomerates. Quartz and microcline grains, and cement composed of finely crystalline siderite and ferruginous dolomite, were encountered in the sandy groundmass of the conglomerates. The Upper Callovian conglomerate (Poddębice PIG 2 borehole) is composed of clasts of brown clayey siderite, brown ferruginous sandstone with bioclasts, grey-brown limestone, and skeletal fossils. Outlines of the bioclasts are poorly visible due to impregnation of the limestones with iron hydroxides; however, they become more easily recognizable by cathodoluminescence analysis. Chamosite or berthierine ooids and goethite ooids have also been recorded.

The Jurassic sandstones (Fig. 5A–E) are represented by fine- to medium-grained, locally coarse-grained varieties and are categorized as quartz and subarkosic arenites and wackes, occasionally sublithic (Pągów IG 1 borehole; Fig. 4). The arenites are conspicuous by an unoriented fabric, while the wackes commonly show a directional fabric accentuated by the arrangement of clay mineral and mica flakes, as well as of organic matter and siderite. Sandstones, accompanied by claystones, mudstones or siltstones, are frequent components of heterolithic deposits. A characteristic feature of most of the sandstones is their relatively monotonous mineral composition. The main component of the grain framework is monocrystalline quartz that predominates over polycrystalline quartz, the content of which usually does not exceed 10 vol.% of rock (Fig. 5A, B). The group of polycrystalline quartz grains includes also clasts of quartzite, quartz schist and chert. The amount of feldspars is ~1 vol.% of rock. Higher feldspar contents (up to 6.0 vol.%) were found in Lower Jurassic sandstones of the Pągów IG 1 and Włoszczowa IG 1 boreholes. The rocks also host clasts of quartz-mica schist, granitoid, volcanic glass, mudstone and mica, and fine carbonaceous debris and scattered organic matter. The Middle Jurassic sandstones often contain bioclasts represented by bivalve and brachiopod shell fragments, bryozoan colonies, crinoid ossicles, and echinoid spines (Fig. 5D). Chamosite or berthierine and goethite ooids are present in places (Fig. 5C). Glauconite grains are found in the Callovian deposits. Pore cement occurs in the arenites, while contact cement is present in the wackes.

Intergranular spaces are filled with a matrix and/or a cement. Quartz cement, accounting for ~10 vol.% of rock, plays the most important role in the Lower Jurassic sandstones, while in the Middle Jurassic sandstones, its content is usually ~2 vol.%. It forms syntaxial overgrowths on quartz grains, filling the pore spaces partially or locally completely (Fig. 5A, B). The boundary between detrital quartz grains and their overgrowth is locally marked by fluid inclusions or iron hydroxides. In the Lower Jurassic sandstones, carbonate cements are represented mainly by siderite (a mineral included in the siderite-magnesite isomorphic series) and ankerite, occasionally by calcite (Table 2). In the Middle Jurassic sandstones, calcite predominates over dolomite. Two generations have been distinguished among the siderites: early and late. The early generation cement is represented by siderite and sideroplesite, which form aggregates of very finely crystalline grains. The late generation siderite is characterized by a higher $MgCO_3$ content than the early diagenetic one, and is represented by sideroplesite. Dolomite and ankerite occur most commonly as isolated euhedral rhombohedral crystals, or they form spar cement. Calcite in the cements of the sandstones commonly contains admixtures of iron and manganese. This indicates that it is a ferruginous variety of calcite. Calcite in the Middle Jurassic sandstones of the Kuyavian area contains small proportions of magnesium, manganese and iron (Maliszewska, 1998). In a CL image, it shows yellow, yellow-orange or reddish luminescence. Authigenic clay minerals are represented by kaolinite, illite, chlorite and illite/smectite mixed-layer minerals. Kaolinite occurs most commonly in the form of platy aggregates visible under scanning electron microscopy as pseudohexagonal crystals creating a characteristic booklet structure. Microscopic observations indicate the occurrence of vermiform kaolinite. Illite crystallites occur most commonly as fibres. Fibrous illite grows on platy illite, quartz cement, and kaolinite. In places, the mineral fills pore spaces in sandstones, reducing its permeability. Authigenic chlorites, which represent a Fe-Mg variety, were observed locally (e.g., sandstones from the Gomunice 13, Pągów IG 1 and Poddębice PIG 2 boreholes). Chlorites in rock samples from the Miechów Trough form rims on quartz grains,

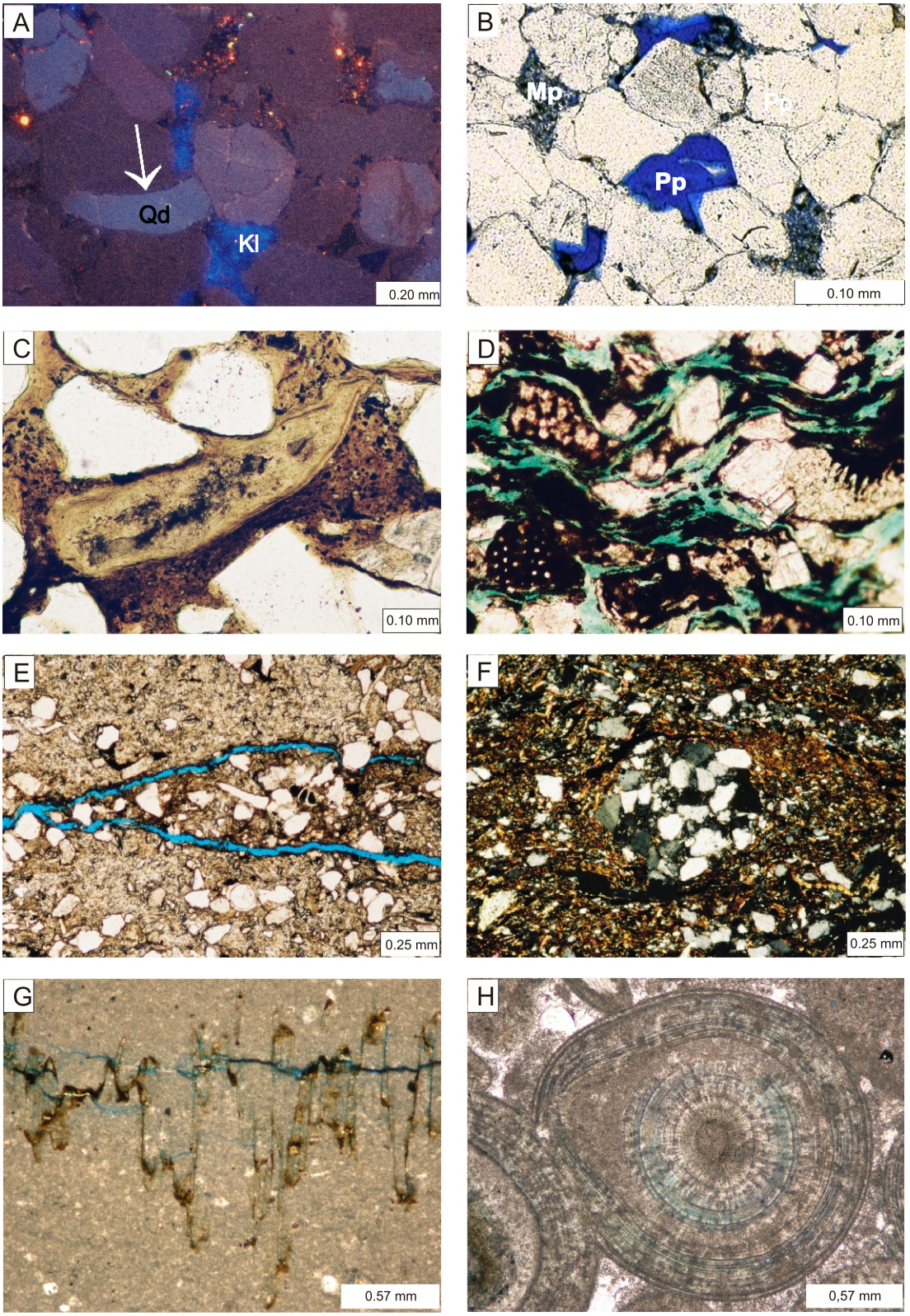

Fig. 5. Photomicrographs in a polarizing microscope (PL) and cathodoluminescence (CL)

A – quartz arenite; dark brown luminescence of authigenic quartz (arrow) and brown and grey-blue detrital quartz grains (Qd), and blue luminescence of kaolinite (Kl). Banachów IG 1 borehole, depth 3338.2 m, Lower Jurassic, CL image; **B** – quartz arenite; primary porosity (Pp) and microporosity (Mp) between kaolinte crystals. Banachów IG 1 borehole, depth 3338.2 m, Lower Jurassic; sample impregnated by blue resin, without analyzer; **C** – berthierine or chamosite ooids flattened by mechanical compaction. Poddębice PIG 2 borehole, depth 3227.7 m, Middle Jurassic, PL, without analyzer; **D** – dolomitic sandstone with bioclasts; visible green flakes of chlorite. Żerechowa 2 borehole, depth 1159.9 m, PL, without analyzer; **E** – microfractures (blue colour) in clayey sandstone. Węgleszyn IG 1 borehole, depth 1726.8 m, Middle Jurassic, sample impregnated by blue resin, PL, without analyzer; **F** – mudstone; visible cross-section through a sand-filled animal burrow. Poddębice PIG 2 borehole, depth 3919.6 m, Middle Jurassic, PL, crossed polars; **G** – mudstone; visible microstylolite zone and a fine crack (blue colour). Secemin IG 1 borehole, depth 970.5 m, Upper Jurassic, sample impregnated by blue resin, PL, without analyzer; **H** – grainstone; visible microporosity within the ooids (blue colour). Jaronowice IG 1 borehole, depth 754.3 m, Upper Jurassic, sample impregnated by blue resin, PL, without analyzer

Table 2

Chemical compositions from microprobe analyses of the carbonates

Borehole	Depth (m)	Point of analysis	$CaCO_3$ mol%	$MgCO_3$ mol%	$FeCO_3$ mol%	$MnCO_3$ mol%	Carbonate type
Lower Jurassic							
Banachów IG 1	3383.1	1 2	56.3 53.7	22.7 21.4	19.7 23.3	1.3 1.6	ankerite ankerite
Madaje Stare IG 1	2472.0	1	53.5	17.2	25.7	3.6	ankerite
Pągów IG 1	1498.3	1 2	50.6 55.3	24.0 17.8	22.2 22.7	3.2 4.2	ankerite ankerite
Secemin IG 1	1331.7	1 2	2.6 96.6	0.8 0.0	93.8 2.7	2.8 0.7	siderite Fe-calcite
Lower Creataceous							
Ponętów 2	1483.6	1	96.5	1.5	2.0	0.0	Fe-calcite
Przybyłów 1	1857.2	1 2	98.7 54.8	0.0 25.9	0.5 18.8	0.8 0.5	Mn/Fe-calcite ankerite
Upper Creataceous							
Młyny 1	1150.1	1	97.8	1.1	0.9	0.2	Fe-calcite

whereas those identified in sandstones from the Łódź Trough more frequently fill the pore space. Mixed-layer illite/smectite minerals have been identified by X-ray studies. They are characterized by illite contents above 90%, indicating a degree of ordering of the illite/smectite structure – R 3 (Horton, 1985; Drits, 1997). Pyrite and hematite occur most commonly in association with organic matter and siderite in clay laminae. Anhydrite cements and aggregates of a green clay mineral showing a chamosite or berthierine composition are found locally in the Middle Jurassic sandstones. The matrix is most commonly composed of a mixture of detrital clay minerals, quartz silt, iron hydroxides, and carbonaceous matter.

Siltstones, mudstones (Fig. 5F) and claystones commonly occur as alternating layers and laminae, forming heterolithic deposits (especially in the Aalenian and Bajocian). These rocks are characterized predominantly by a directional fabric, accentuated by the parallel arrangement of laminae of clay minerals and micas, which are commonly accompanied by organic matter and finely crystalline siderite, iron hydroxides, carbonized plant detritus, and local pyrite. The mineral composition of the mudstones is the same as that of the sandstones. Locally, radial siderite spherulites and ankerite cement are observed. On the basis of X-ray analysis (Fig. 6), illite, kaolinite and chlorite,

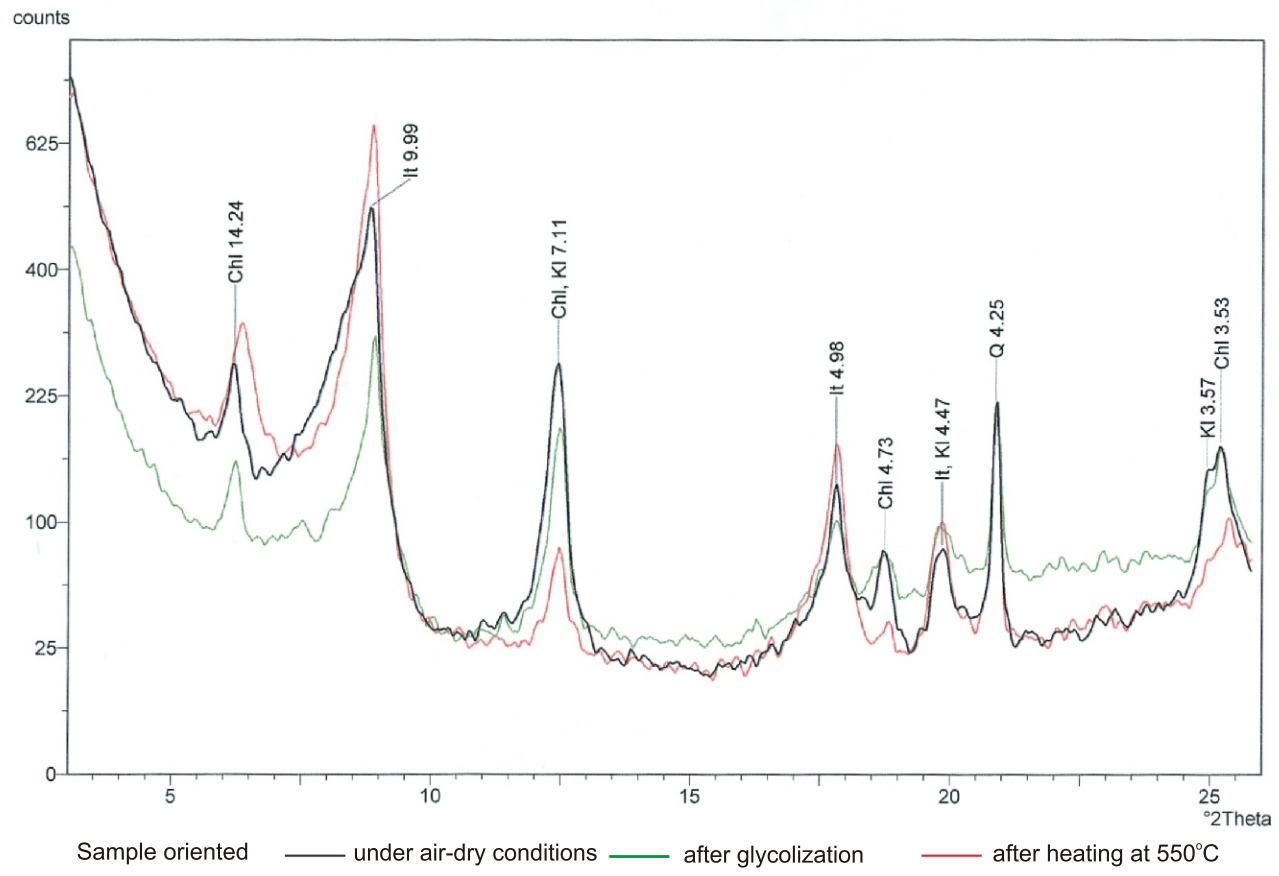

Fig. 6. XRD diagram of the clay fraction <0.2 μm of the Lower Jurassic mudstone

Chl – chlorite, It – illite, Kl – kaolinite; Q – quartz. Banachów IG 1 borehole, depth 3301.5 m

and local illite/smectite mixed-layer minerals containing 85-90% of illite, similar to that found in the claystones (Krystkiewicz, 2008), have been identified in the mudstones.

Carbonate rocks (Fig. 5G, H) dominate in the Upper Jurassic, but occur also in the Middle Jurassic. These are chiefly limestones, occasionally dolomitic and sandy, represented by grainstones, mudstones, wackestones, packstones, floatstones, rudstones and boundstones. Dolomite and siderite rocks are less common. Among the granular constituents, bioclasts (including detritus of ostracods, algae and fish, brachiopod and bivalve shell fragments, crinoid ossicles, sponge spicules), ooids (Fig. 5H), oncoids and detritus represented by quartz silt, small lithoclasts, pyrite and glauconite are commonly present. Some bioclasts, partially dissolved, are filled with calcite or dolomite spar, chalcedony, pyrite, anhydrite and celestine. Microstylolites and minute fractures are commonly observed (Fig. 5G). In the carbonate rocks, isopachous bladed cements and blocky cements, filling voids in the rock, have been distinguished. Cathodoluminescence analysis shows that these rocks are generally characterized by weak luminescence. In non-fractured rocks, only bioclast grains show more intense luminescence against a brown background of almost pure calcite. The rocks that are fractured and healed with blocky cements commonly show a coloured banded structure in cathodoluminescence, which is due to varying contents of mainly Mn and Fe admixtures. Apart from carbonate cements, anhydrite and siliceous cements are also observed. Most of the dolomites are massive, commonly recrystallized, and contain barely recognizable shell fragments. Some contain goethite ooids and an admixture of mud, silt or sand-sized quarts grains. Sideritic rocks are observed in the Bajocian and Upper Bathonian. These are mostly clayey siderites composed of siderite micrite and microspar, impregnated with clay minerals. Some of them contain fine quartz grains, organic matter, iron hydroxides, and pyrite.

CRETACEOUS (FIG. 7)

In the boreholes drilled in the Łódź Trough, conglomerates are found in the Hauterivian and Aptian-Albian (Raczyńska, 1979). They are composed of quartz pebbles and clasts of clay-ferruginous rocks with a coarse-grained sandy matrix, which has a quartz arenite composition (Raczyńska, 1973). Pebbles of vein quartz, quartzite and quartzite schist, and rarely of quartz-mica and quartz-feldspar rocks, have also been reported. The groundmass consists of fine- to medium-grained sandy matrix cemented by clay minerals, iron hydroxides and pyrite. In places, there are gravel-sized clasts of limestone, with a sandy and calcareous matrix. In the Upper Albian conglomerates, clasts of metamorphic schist, effusive rocks and poorly rounded flint fragments have also been identified. In addition, the rocks contain partially silicified oyster and brachiopod remains, spines and plates of echinoids, and crinoid ossicles. The Cenomanian conglomerates are rich in phosphorites, organic remains, and quartz and glauconite grains, while the Santonian conglomerates are composed of pebbles covered with glauconite, embedded in a marly cement containing numerous phosphorite concretions and glauconite (Rutkowski, 1965).

The thickest Lower Cretaceous sandstone (Fig. 7A–C) units are found in the Barremian-Middle Albian interval. In the Miechów Trough, sandstones occur only in the Albian (Jurkiewicz, 1974a, 1976a, b, 1994). In the Upper Cretaceous, sandstones are found in the Santonian and Campanian of the Łódź Trough and in the Cenomanian and Maastrichtian of the Miechów Trough. The sandstones are mostly poorly cohesive fine- to medium-grained rocks. These are quartz arenites and wackes, subordinately sublithic arenites (Fig. 4). Monocrystalline quartz grains are the primary constituent; polycrystalline quartz grains are less common (Fig. 7A). Very thin clay-ferruginous rims are locally present on the grains. Lithoclasts are represented by fragments of quartzite and crystalline schist, siliceous rocks, clay-ferruginous rocks, single pebbles of ferruginous sandstones and mudstones, and granitoid rocks. Feldspar grains are rare (~2 vol.%). Potassium feldspars are present, mostly of microcline composition, while plagioclases are much rarer. Abundant glauconite aggregates are a frequent component of quartz-glauconitic sandstones (Fig. 7B). In the Upper Cretaceous sandstones from the Pągów IG 1 borehole, the glauconite content exceeds 20 vol.% of rocks. Locally, very fine-grained sandstones with biotite and chlorite are observed. Ferruginous ooids, composed of chamosite, goethite or hematite, less frequently of siderite and apatite, occur in places. Bioclasts and small clasts of carbonaceous plant remains are occasionally found. The sandstones contain a clay-ferruginous matrix and cements. Quartz cement occurs as overgrowths on quartz grains. The Upper Cretaceous sandstones of the Miechów Trough are also cemented by chalcedony. The content of siliceous cements is up to 5–6 vol.% of rock. Carbonate minerals (Table 2) in the sandstones form pore cement. The most abundant calcite cement found in the Santonian and Campanian sandstones is poikilotopic cement (>30 vol.% of rock) which contains relics of bioclasts. There is also calcite, which is orange and brown in cathodoluminescence. Another component is siderite, developed as highly elongated crystals scattered in the intergranular spaces or as spherulites. It also forms pore cement. Some of the sandstones are cemented by Fe/Mg-chlorite, most frequently developed as rims consisting of plates arranged perpendicular to grain surfaces (Fig. 7C). Clay minerals are represented by kaolinite. Vermiform kaolinite is encountered within clay-ferruginous cement, while blocky kaolinite occurs in intergranular spaces. Phosphates are occasionally observed.

Siltstones and mudstones (Figs. 7D and 8) are composed of clay minerals (illite, smectite, kaolinite, chlorite), iron oxides and hydroxides, and granular material of the clay and silt fractions. Granular components are represented by quartz, glauconite, mica flakes, feldspars, lithoclasts and rare ferruginous ooids. Bioclasts (Fig. 7D) are locally scattered and occur as thin layers. In addition, partially pyritized carbonaceous plant detritus is found. The rocks contain calcite or siderite impregnations. A particular variety of these rocks is quartz siltstone cemented by carbonate spar. In places, these sediments show abundant bioturbation.

Parting-lineated claystones and clay shales are composed of organic matter impregnated by clay minerals and significant amounts of iron compounds, which give them a dark grey and almost black colour. A special variety is greenish chamosite claystone (Sarnów IG 1, Koło IG 3, Banachów IG 1) containing ooids.

Ferruginous rocks occur mostly in the form of layers and concretions. Their light brown and greenish-brown colours are due to the presence of iron oxides and hydroxides. The siderite rocks are composed of micro- and locally finely crystalline siderite of the siderite-magnesite isomorphic series, sideroplesite and pistomesite (Połońska, 1999a), as well as clay minerals and disseminated iron hydroxides. These rocks contain siderite and siderite-goethite ooids, ferruginous rock clasts, and rarely biodetritus. In addition, kaolinite and berthierine have been reported (Połońska, 2007).

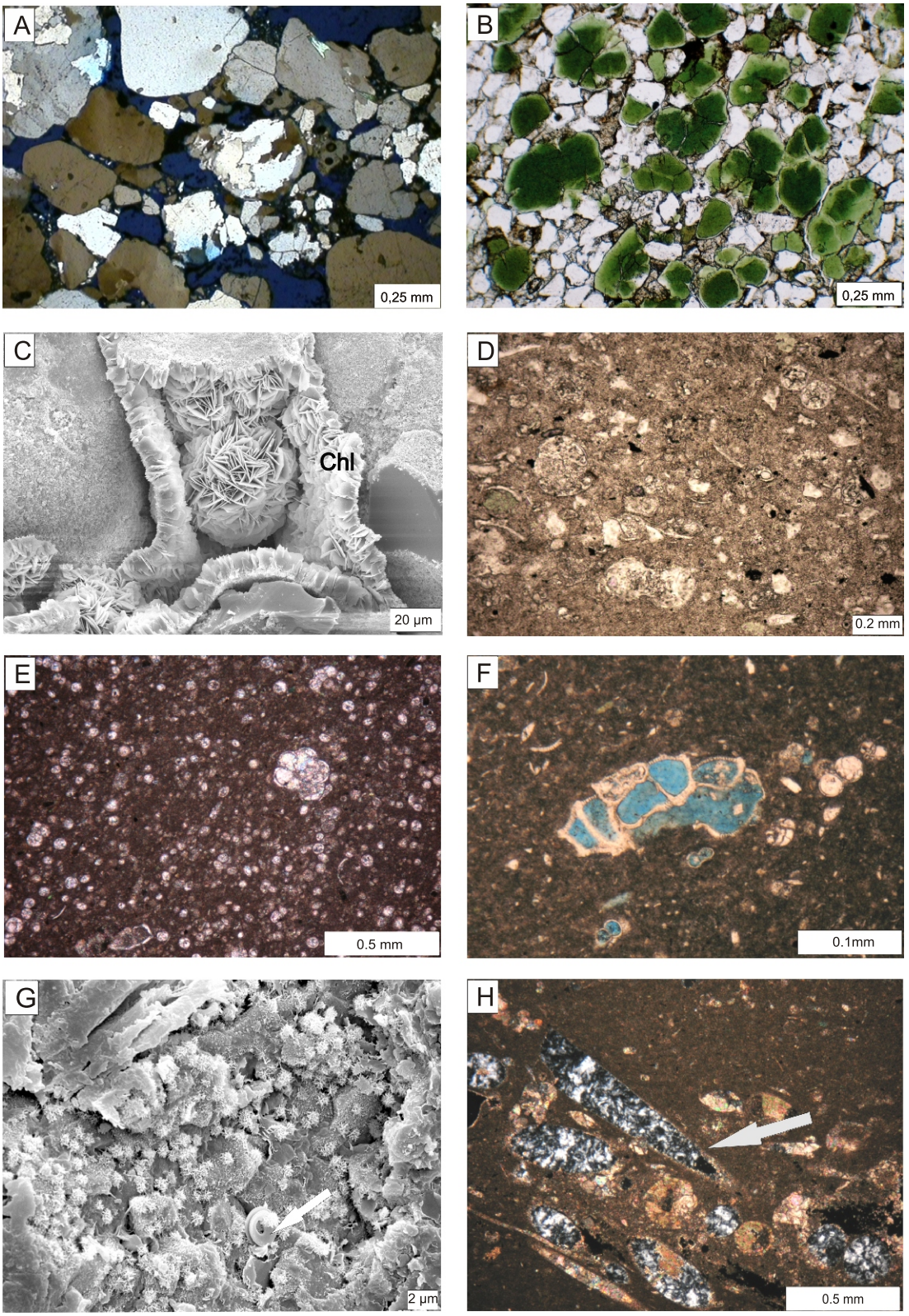

Fig. 7. Photomicrographs in a polarizing microscope (PL) and ascanning electron microscope (SEI)

A – polycrystalline quartz grains (in the centre of the photograph) in coarse-grained sandstone. Poddębice PIG 2 borehole, depth 2207.5 m, sample impregnated by blue resin, Lower Cretaceous, PL, without analyzer; **B** – quartz-glauconite sandstone. Pagórki IG 1 borehole, depth 1059.0 m, Lower Cretaceous, PL, without analyzer; **C** – chlorite (Chl) rims and rosettes in sandstones. Banachów IG 1 borehole, depth 2354.6 m, Lower Cretaceous, SEI image; **D** – calcareous mudstone with bioclasts. Młyny 1 borehole, depth 840.5 m, Upper Cretaceous, PL, without analyzer; **E** – organodetrital limestone; a calcisphere and a foraminifer test are visible. Koło IG 3 borehole, depth 1634.9 m, Upper Cretaceous, PL, crossed polars; **F** – marly limestone with a foraminifer test with an internal void (blue colour). Pągów IG 1 borehole, depth 387.3 m, Upper Cretaceous, sample impregnated by blue resin, PL, without analyzer; **G** – fragment of opoka-rock; coccolith (arrow) and opal CT lepispheres are visible. Poddębice PIG 2 borehole, depth 617.9 m, Upper Cretaceous, SEI image; **H** – opoka-rock with sponge spicules filled by chalcedony (arrow). Koło IG 3 borehole, depth 807.6 m, Upper Cretaceous, PL, crossed polars

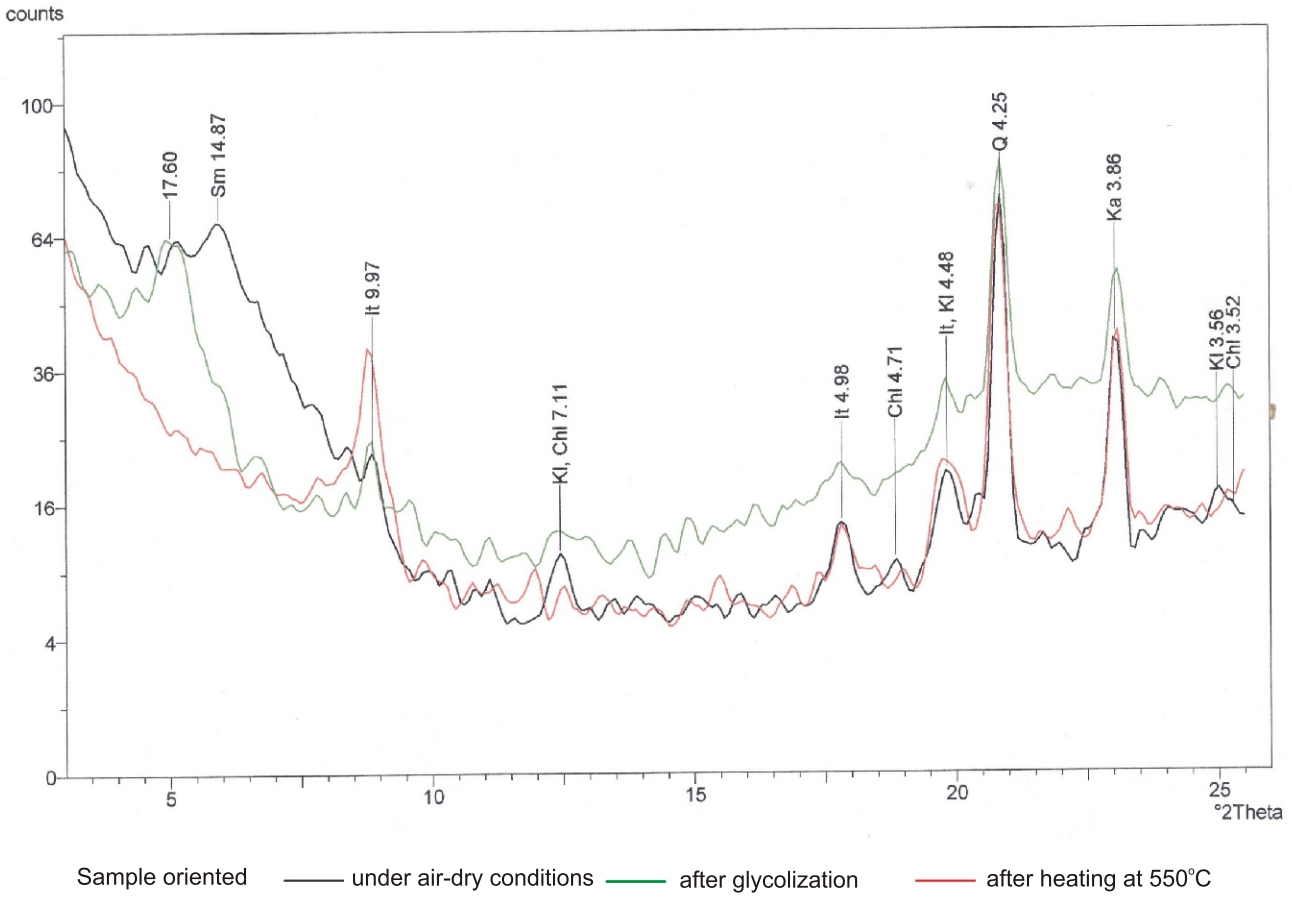

Fig. 8. XRD diagram of the clay fraction <0.2 μm of Upper Cretaceous calcareous mudstone

Chl – chlorite, It – illite, Ka – calcite, Kl – kaolinite; Sm – smectite, Q – quartz. Młyny 1 borehole, depth 840.5 m

Limestones (Fig. 7E) are a common Cretaceous lithofacies, comprising pelitic and granular varieties. Mudstones are predominant, while wackestones, packstones and rudstones are found less frequently. Granular material is dominated by faunal remains, including ostracod shells, coquina-forming accumulations of bivalve and gastropod shells, foraminifera (Fig. 7E), echinoderms, echinoid spines, and fish remains. Microfossils are represented by skeletons of radiolaria and diatoms. Besides bioclasts, there are peloids and intraclasts composed of micritic, locally ooidal and bioclastic limestone, and subordinate calcitic ooids. The limestones are classified as organodetrital, peloidal and intraclastic varieties. Microcrystalline calcite is their primary constituent. Granular limestones also contain calcite spar, forming basal and pore cements. In cathodoluminescence images, the calcite cement is orange or brownish, indicating the presence of a ferruginous variety with a small admixture of manganese. Larger calcite crystals reveal a banded structure. Micrite and bladed rims on carbonate grains are observed. Syntaxial overgrowths on echinoderm remains are rare. Dolomite crystals occur in dispersed form or in larger clusters that form minor interbeds and streaks. Ankerite cement accounts for a small proportion. In places, larger pore spaces are filled with kaolinite.

Marly varieties of limestone (Fig. 7F), locally silicified, have been encountered in some borehole sections. Locally, they are characterized by a nodular texture and the presence of stylolites.

Apart from these rock types, there are also marls, opokas (Fig. 7G, H), gaizes, and sulphate rocks composed of anhydrite, gypsum and, less frequently, celestine.

POROSITY

TRIASSIC

Buntsandstein deposits of the Łódź-Miechów Trough are represented predominantly by impermeable siltstone, mudstone and claystone units. The sandstones occur as variably thick intercalations and interbeds and show increased porosity and permeability values (Table 3). The porosity, planimetrically measured in sandstones from some boreholes, ranges from 0 to 27 vol.% of the rock. Porosity values exceeding 20% were recorded in samples from the Brzegi IG 1, Gomunice 12 and Pągów IG 1 boreholes, and values exceeding 10% in the Gidle 2, Gomunice 13 and Secemin IG 1 boreholes. Computer image analysis shows that the intergranular space of the samples studied is variably developed (Appendix 1).The percentage distribution of micropore length reveals that ~98–99% of the pores are in the 0.001–0.01 mm size range. The width of >99% of the pores is also in the size range of 0.001–0.01 mm. The petrophysical data show that the maximum values of porosity and permeability were recorded in the Brzegi IG 1 borehole - ~17% and >100 mD, respectively (Table 3). Other pore space parameters of the sandstones from the Brzegi IG 1 borehole also show good reservoir properties. The amount of pores above 1 μm in size is the greatest here (~80%), indicating a macroporous intergranular space. These sandstones are characterized by the highest threshold diameter value (30 μm) within the Lower Triassic deposits. The differences in hysteresis effect values (26–59%) indicate a heterogeneous development of the pore space, while the lowest values <30% confirm their

Table 3

Petrophysical features of selected sandstone and carbonate samples

Borehole	Age	Depth	Type of rock	Grain density	Effective porosity	Bulk density	Porosimeter density	Porosimeter porosity	Average capillary	Specific surface	Pores >1 um	Threshold diameter	Hysteresis	Permeability
		[m]		[g/cm^3]	[%]	[g/cm^3]	[g/cm^3]	[%]	[μm]	[m^2/g]	[%]	[μm]	[%]	[mD]
Brzegi IG 1	T1	1498.9	sandstone	2.71	4.93	2.67	2.54	4.74	0.05	1.54	10.00	0.80	59	8.45
Brzegi IG 1		1532.2	sandstone	2.64	17.46	2.62	2.17	17.12	0.65	0.49	82.00	30.00	28	103.52
Brzegi IG 1		1558.4	sandstone	2.64	17.09	2.65	2.19	17.26	0.56	0.57	81.00	30.00	26	138.59
Gidle 2		2095.3	sandstone	2.65	16.83	2.61	2.19	16.18	0.15	2.00	50.00	5.00	65	0.01
Gidle 2		2098.2	sandstone	2.68	4.50	2.60	2.49	4.17	0.05	1.43	14.00	0.80	40	8.68
Gidle 2		2151.2	sandstone	2.65	12.93	2.56	2.26	11.86	0.14	1.49	50.00	10.00	62	0.01
Gomunice 9		2264.3	sandstone	2.66	7.87	2.67	2.46	7.95	0.12	1.04	40.00	3.00	63	1.58
Gomunice 12		2156.6	sandstone	2.65	10.98	2.61	2.33	10.56	0.13	1.38	30.00	2.00	64	0.01
Gomunice 12		2358.1	sandstone	2.64	13.18	2.60	2.27	12.67	0.25	0.90	69.00	15.00	60	0.01
Gomunice 13		2453.5	sandstone	2.66	10.60	2.62	2.36	10.19	0.16	1.07	58.00	4.00	67	1.52
Milanów 2		2073.3	sandstone	2.70	2.86	2.65	2.57	2.72	0.04	1.18	20.00	0.50	46	0.01
Milanów 2		2075.3	sandstone	2.69	7.71	2.62	2.43	7.21	0.13	0.90	65.00	10.00	63	0.00
Pągów IG 1		2239.0	sandstone	2.66	6.94	2.65	2.47	6.87	0.17	0.65	22.00	2.00	50	27.24
Pągów IG 1		2332.5	sandstone	2.66	12.24	2.65	2.33	12.12	0.13	1.56	14.00	2.00	61	4.63
Pągów IG 1		2403.1	sandstone	2.66	11.40	2.64	2.34	11.18	0.09	2.22	7.00	1.00	53	0.83
Zamoście 1		2309.5	sandstone	2.73	0.00	2.46	2.46	0.00	0.00	0.00	0.00	0.00	0	0.82
Gidle 2	T2	1788.3	carbonate	2.73	26.35	2.79	2.01	28.03	1.03	0.54	69.00	10.00	84	n.d.
Gomunice 9		1455.8	carbonate	2.81	16.34	2.82	2.35	16.50	0.31	0.92	8.00	1.00	71	0.429
Gomunice 13		2001.25	carbonate	2.74	0.45	2.75	2.74	0.45	0.03	0.26	45.00	0.00	58	0.5
Pągów IG 1		2134.0	carbonate	2.76	5.15	2.63	2.51	4.56	0.04	2.05	5.00	0.10	65	0.01
Radziątków 7		2560.0	carbonate	2.71	15.43	2.72	2.30	15.59	0.06	4.38	5.00	0.20	93	0
Radziątków 7		2572.0	carbonate	2.68	7.55	2.68	2.48	7.55	0.09	1.39	6.00	0.30	80	<0.01
Radziątków 7		2580.0	carbonate	2.73	10.71	2.64	2.38	9.83	0.23	0.71	18.00	2.00	79	n.d.
Gomunice 13	T3	1330.0	sandstone	2.70	11.74	2.66	2.36	11.29	0.23	0.85	51.00	10.00	67	4.34
Gomunice 13		1335.5	sandstone	2.69	3.53	2.59	2.51	3.21	0.02	3.16	9.00	0.05	69	n.d.
Gomunice 13		1550.0	sandstone	2.77	1.56	2.67	2.63	1.42	0.02	1.39	18.00	0.02	67	n.d.
Banachów IG 1	J1	3279.2	sandstone	2.65	8.33	2.61	2.41	8.01	0.31	0.42	44.00	2.00	67	0.961
Banachów IG 1		3338.2	sandstone	2.65	6.79	2.64	2.46	6.72	0.20	0.55	26.00	2.00	54	2.971
Banachów IG 1		3383.1	sandstone	2.63	9.75	2.69	2.41	10.37	1.29	0.13	83.00	30.00	31	n.d.
Gomunice 13		1035.0–1041.0	sandstone	2.64	23.07	2.64	2.03	23.07	0.92	0.49	84.00	45.00	23	1109.895
Madaje Stare IG 1		2451.5	sandstone	2.69	16.49	2.60	2.21	15.13	4.34	0.06	95.00	30.00	8	n.d.
Madaje Stare IG 1		2472.0	sandstone	2.67	11.61	2.61	2.34	10.53	3.60	0.05	95.00	40.00	11	n.d.
Pągów IG 1		1474.4	sandstone	2.68	16.34	2.66	2.24	16.02	0.22	1.29	56.00	10.00	n.o.	82.810
Pągów IG 1		1526.0	sandstone	2.67	26.69	2.65	1.95	26.17	1.09	0.49	85.00	20.00	n.o.	311.31
Włoszczowa IG 1		1692.0	sandstone	2.66	10.65	2.61	2.35	10.14	0.09	1.93	7.00	0.70	n.o.	0.582
Zgierz IG 1		2405.0–2407.0	sandstone	2.64	15.96	2.63	2.21	15.80	5.43	0.05	86.00	20.00	55	43.251
Zagość -2	J2	1137.0	sandstone	2.70	7.50	2.62	2.44	6.94	0.05	2.48	9.00	0.50	48	0.01
Zagość 2		1143.0	sandstone	2.68	7.82	2.62	2.42	7.38	0.06	1.92	14.00	0.90	41	0.1
Zagość 2		1144.0	sandstone	2.70	2.44	2.65	2.59	2.32	0.03	1.32	16.00	0.20	46	1.27
Jaronowice IG 1	J3	710.6	carbonate	2.70	4.93	2.70	2.56	4.93	0.07	1.17	4.00	0.20	73	0.0
Kostki Małe 2		940.5	carbonate	2.70	6.94	2.67	2.49	6.74	0.05	2.41	3.00	0.10	76	0.1
Kostki Małe 2		944.0	carbonate	2.69	2.85	2.68	2.60	2.82	0.02	2.25	7.00	0.05	78	<0.01
Secemin IG 1		768.9	carbonate	2.71	13.72	2.69	2.33	13.45	0.41	0.56	55.00	4.00	42	n.d.
Węgleszyn IG 1		1078.5	carbonate	2.70	5.73	2.70	2.54	5.73	0.09	0.98	4.00	0.40	69	n.d.
Włoszczowa IG 1		1067.0	carbonate	2.70	4.39	2.66	2.55	4.22	0.16	0.43	8.00	0.70	68	n.d.
Zagość 2		954.0	carbonate	2.69	1.21	2.69	2.66	1.21	0.02	0.80	20.00	0.10	80	0.269
Banachów IG 1	K1	2354.6	sandstone	2.69	15.00	2.63	2.26	14.15	0.11	2.36	51.00	4.00	70	4.06
Poddębice PIG 2		2216.3	sandstone	2.65	18.18	2.65	2.16	18.18	3.90	0.09	90.00	90.00	7	n.p.
Poddębice PIG 2		2257.6	sandstone	2.66	28.25	2.67	1.91	28.54	0.53	1.14	72.00	30.00	57	n.p.

Tabl. 3 cont.

Ponętów 2		1564.5	sandstone	2.66	18.84	2.67	2.16	19.03	1.17	0.30	91.00	50.00	14	587.62
Sarnów IG 1		1751.4	sandstone	2.64	17.04	2.64	2.19	17.04	1.08	0.29	85.00	40.00	21	114.48
Strzelno IG 1		1385.7	carbonate	2.75	2.87	2.65	2.58	2.61	0.16	0.25	28.00	2.00	78	0.507
Strzelno IG 1		1391.7	carbonate	2.85	4.27	2.81	2.70	4.11	0.03	1.86	6.00	0.20	79	0.01
Koło IG 1	K2	829.7	sandstone	2.65	5.58	2.61	2.47	5.56	2.31	0.07	74.00	10.00	73	13.046
Poddębice PIG 2		617.9	opoka	2.60	23.13	2.50	1.98	21.03	0.02	19.01	2.00	0.20	52	0.01
Poddębice PIG 2		1208.4	marl	2.65	10.70	2.56	2.31	9.82	0.03	5.82	3.00	0.10	70	0.010
Strzelno IG 1		150.1	gaize	2.58	42.21	2.52	1.51	39.82	0.05	20.87	1.00	1.00	34	0.01

T1 – Lower Triassic, T2 – Middle Triassic, T3 – Upper Triassic, J1 – Lower Jurassic, J2 – Middle Jurassic, J2 – Upper Jurassic; K1 – Lower Creataceous, K2 – Upper Creataceous; n.d. – no data, n.p. – non-permeable

good reservoir properties. Sandstones from the Gomunice area and from the Gidle 2 borehole are characterized by porosity >10% and permeability of ~0.01–1.5 mD.

In the Middle Triassic, carbonate rocks: dolomitized peloidal grainstones from the Gidle 2 borehole, dolomites from the Gomunice 9 borehole, and grainstones from the Radziątków 7 borehole, are characterized by a total porosity ranging from 7 to 26% and are poorly permeable (from 0 to ~0.5 mD; Table 3). The rocks in the Gidle 2 borehole have 69% of pores >1 μm, threshold diameter 10 μm and hysteresis 84%. Computer image analysis data indicate that the pores are elongated (Appendix 1). Rocks from the other boreholes are characterized by microporous pore spaces and low permeabilities. The amount of pores larger than 1 μm usually does not exceed 20%, and the threshold diameter values are most often <1 μm. The hysteresis value is in the range of 71–93%.

Some beds of the Upper Triassic sandstones and sandy mudstones exhibit evident primary intergranular porosity, but micropores usually predominate over macropores.Computer image analysis shows that the average pore length varies between 0.00313 and 0.00600 mm and the width is between 0.00187 and 0.00198 mm (Appendix 1). The pores, whose length and width are within a range of 0.01–0.001 mm, account for approximately 99%. Upper Triassic fine-grained sandstones from the Gomunice 13 borehole were subjected to porosimetric determinations (Table 3). These rocks are characterized by a total porosity ranging from 1 to ~12%, and a permeability ranging from 0.5 to 4.34 mD. The amount of pores >1 μm is from 9 to 51%, the threshold diameter reaches a maximum of 10 μm, and the hysteresis value is ~68%.

JURASSIC

In the Lower Jurassic sandstones the porosity measured in thin sections ranges from 2 to 31 vol.% of rock, with an average of ~15 vol.%. Computer image analysis shows that macropores (>0.001 mm) dominate over micropores (<0.001 mm) in the pore space of the rocks (Appendix 1). The sandstones with a porosity of around 15% contain more pores >0.01 mm in length and width compared to the sandstones with a porosity of less than 10%. The total porosity of the sandstones ranges from 5 to ~27%, and the permeabilities are from 0.582 to 1109.895 mD (Table 3). The highest porosity values (>15.0%) were found in sandstone samples from the Gomunice 13, Madaje Stare IG 1, Pągów IG 1 and Zgierz IG 1 boreholes. Their porosimetric parameters show that the percentage of >1 m pores varies from 7 to 95% (80–95% for most samples). The threshold diameter is in the range of 1–90 m; most frequently around 35 m. The hysteresis value ranges from 4 to 67%, usually ~25%.

The Middle Jurassic sandstones are characterized by porosities ranging from 2 to >20%, reaching in places 30 vol.% of the rock, as measured in thin sections. Computer image analysis indicates that ~97.7–98.6% of pores are 0.01–0.001 mm in length and width (Appendix 1). Sandstones from the Zagość 2 borehole are characterized by a total porosity in the range of 2 - ~8%, and a permeability of 0.1–1.27 mD (Table 3). The percentage of >1 μm pores varies from 9 to 16%, the threshold diameter does not exceed 1 μm, and the hysteresis value is ~45%. Claystones, siltstones and marls are generally poorly porous and impermeable. Barely porous and poorly permeable rocks are represented by limestones and clay siderites.

The Upper Jurassic carbonates may be porous to varying degrees, but their permeability is generally low. The porosity of these rocks measured in thin section is usually a few per cent (1–7 vol.% of rock). Petrophysical studies of the carbonates show very low permeabilities (<0.01 to 0.269 mD) in most samples, and their total porosity ranges from 0.61 to 6.94% (Table 3). The only sample that shows very good filtration capacity, total porosity of ~14%, and permeability of 331.41 mD is the one from a depth of 768.9 m in the Secemin IG 1 borehole. Porosimetric analysis showed a high content of pores with diameters larger than 1 μm (55%) and a relatively low hysteresis value (42%). The threshold diameter value is 4 μm.

CRETACEOUS

The Lower Cretaceous sandstones are characterized mostly by good porosity, while the arenites with a small amount of clay matrix have very good porosity. The results of planimetric analysis show that the proportion of pores in the arenites range from ~2 to ~20 vol.% of the rock, and in the wackes it is up to ~11 vol.%. The length and width of the pores were determined using computer image analysis (Appendix 1). Most of the pores are characterized by length and width less than 0.01 mm. The pore length is occasionally more varied than the width, which is usually <0.02 mm. The petrophysical data show that the total porosity of the sandstones varies from 15.0 to 28.25%, while the permeability values range from 114.48 to 587.62 mD (Table 3). Due to the limited technical capabilities of the apparatus, permeability measurements have not been obtained in poorly compacted sandstones, which suggests their higher filtration capacity. The average capillary ranges from 0.53 to 3.90 μm, and the specific surface area varies from 0.09 to 1.14 m^2/g. The proportion of pores >1 μm is high (51–90%), and the threshold diameter generally greater than 30 μm, reaching 90 μm. The hysteresis typically ranges from 7 to 57%.

Petrophysical studies of the Berriasian limestones show that their porosity is 2–4%, and their permeability >0.507 mD (Table 3). According to porosimetric studies the content of

pores >1 μm ranges from 6 to 28%, with the threshold diameter from 0.2 to 2 μm. The hysteresis is high and ranges from 78 to 79%. Porosimetric analysis of gaizes, opokas and marls reveals microporosity in these rocks and very poor filtration capacities.

The Upper Cretaceous sandstones are characterized by porosities in the range of 0–38 vol.% of rock, as measured from planimetric analysis. The percentage distribution of length and width values, as determined by computer image analysis, shows that they cluster predominantly within intervals of less than 0.01 mm (Appendix 1). Most often, the length values vary more than the width values. The results of petrophysical studies of carbonate-cemented quartz arenite are given in Table 3. The rock is characterized by a total porosity of 5%, a high hysteresis of 73%, and a permeability of ~13.0 mD. The Cenomanian and Maastrichtian sandstones in the Miechów Trough show porosities ranging from 9 to ~33%, and permeabilities from >100 mD to a maximum of 2073 mD (Jurkiewicz, 1974a,b, 1976a,b, 1994).

The carbonate-marly rocks are represented by limestones, marls, and siliceous carbonates: opokas and gaizes. They are characterized by porosities ranging from 1 to 39%, and permeabilities locally exceeding 100 mD (Jurkiewicz, 1994). Gaizes and opokas exhibit a higher total porosity of 42% and 23%, respectively, than marls (~11%), but their permeabilities are at the same, very low level of 0.01 mD (Table 3). The petrophysical parameters of these rocks are similar, as follows: content of pores >1 μm is 1–3%, threshold diameter is 0.1–1 μm, and hysteresis is from 34 to 70%.

DIAGENETIC PROCESSES

SILICICLASTIC ROCKS

Siliciclastic rocks from the Łódź and Miechów troughs show the effects of a number of diagenetic processes: mechanical and chemical compaction, cementation, replacement, dissolution, alteration and neomorphism.

The earliest post-depositional process is burrowing. This is manifested by disturbance of sedimentary structures, most often seen in fine-grained sandstones and mudstone-sandstone heterolithic depositss (e.g., clayey mudstones from the Poddębice PIG 2 borehole, Middle Jurassic). Mechanical compaction started shortly after deposition and resulted in a tighter packing of detrital material. This process was responsible for the occurrence of more abundant intergranular straight and point contacts and for the bending and fracturing of mica flakes or clay laminae. Under pressure, deformation of more ductile grains, such as ferruginous ooids and glauconite aggregates, took place. Chamosite or berthierine ooids, which do not have rigid cores, were stretched to form spastolites. Glauconite has locally been compressed between the more rigid grains. The effect of chemical compaction as concavo-convex intergranular contacts in the sandstones was observed rarely.

Cementation in the siliciclastic deposits was a common process. Carbonate cements (calcite, dolomite, ankerite, siderite) and quartz cements are the most abundant. Calcite is a significant constituent of the carbonate cements. The earliest manifestation of cementation processes comprises fine calcite rims, which were found locally in the Middle Jurassic sandstones. Two calcite generations have been distinguished: an earlier, calcite cement, and a later cement, which is rich in Mn compared to the first generation. Pure calcite has been identified only in the Lower Triassic sandstones. Mn-calcite occurs in all Mesozoic siliciclastic deposits of the Łódź and Miechów troughs. Dolomite occurs either as subhedral crystals filling pore spaces or as rhombohedra, commonly showing a zonal structure. Ankerite is rare and usually forms outer parts of Fe-dolomite crystals.The Jurassic sandstones also contain siderite (a mineral of the siderite-magnesite isomorphic series) represented by two generations (Kozłowska and Krystkiewicz, 2012; Krystkiewicz et al., 2012). Early generation siderite is represented by siderite and sideroplesite, while late generation siderite, characterized by a high-magnesium content, is represented by sideroplesite. Significant accumulation of fine rhombohedra of sideroplesite resulted in both the local formation of clayey siderites and sideritic cementation of coquinas.

Another important component of the cements, especially in quartz arenites, is authigenic quartz. It occurs as overgrowths on detrital quartz grains or it fills pore space. Chalcedony cement was also noted in the Albian sandstones of the Miechów Trough.

In places, anhydrite cement is observed. Anhydrite occurs in the form of small plates, occasionally arranged in a fan-like pattern, some accompanied by gypsum plates. Anhydrite is found most often in the Keuper Gypsum Beds, especially as aggregates in dolomites and claystones.

Authigenic clay minerals are represented by frequent kaolinite, chlorite and illite. Kaolinite occurs most commonly as curvilinear aggregates called “vermiform” in pore space. Chlorites were occasionally observed, mainly as rims on detrital grains or as aggregates filling pore spaces. Fibrous illite filled intergranular, intragranular and intracrystalline spaces in the sandstones. The Jurassic and Cretaceous deposits also contain concentrations of green or brown clay mineral, which is chamosite and/or berthierine in composition. In addition, authigenic feldspar overgrowths on feldspar grains are visible in the Triassic sandstones.

Mineral replacement is associated with the cementation process in the deposits. Their metastable components were most easly replaceable by carbonates. The most frequently replaced grains were feldspars, less frequently micas, lithoclasts and quartz. Replacement of quartz cement and authigenic kaolinite is visible. In places one carbonate mineral replaces another.

Within the Middle Jurassic siderite-rich layers the replacement of berthierine or chamosite ooids and calcite bioclasts by siderite or ankerite were frequently observed (Maliszewska, 1998).

In the siliciclastic deposits, the phenomenon of diagenetic dissolution affected detrital grains (feldspar, mica) and cements (carbonates).

Argillization of feldspar grains and mica flakes is the most commonly observed effect of diagenetic alteration. The products of this process are clay minerals such as kaolinite, chlorite and, to a lesser extent, illite. Chloritization of biotite and partial alteration of siderite into iron hydroxides are equally common. Some of the authigenic kaolinite grains in the sandstones may have been formed following the alteration of feldspars or micas.

CARBONATE ROCKS

The carbonate deposits show effects of mechanical and chemical compaction. Mechanical compaction caused packing and deformation (also fracturing) of granular material and the formation of numerous compaction fissures. The result of chemical compaction is deformation of grains at intergranular contacts, and the formation of straight or concavo-convex contacts. Stylolitization processes indicate significant dissolution of the rocks. Stylolites can provide circulation paths for solutions causing dolomitization (Radlicz, 1966). In the material studied,

however, only some of the stylolites proved to be preferential zones for circulating solutions. The others appear to be completely sealed by clay matter characteristic of these zones.

Carbonate cementation has developed in several stages. The predominant carbonate mineral is calcite, which forms fine crystals, isopachous bladed cements and blocky cements, which occluded the pore space. Dolomite, ankerite and siderite are also present. In addition to carbonate cements, anhydrite and siliceous cements are observed.

In the carbonate deposits, replacement processes, mainly dolomitization and silicification, were important. Dolomitization processes were significant in the Muschelkalk carbonates. Early diagenetic dolomitization of calcareous muds took place in an evaporitic environment. Later dolomitization produced rocks encrusted with dolomite rhombohedra, and, in extreme cases, crystalline dolomites. Parts of bio- and lithoclasts were subject to silicification. Silicification processes are observed predominantly in sponge boundstones and granular rocks containing sponge fragments. Other bioclasts, including belemnites, and fragments of echinoderm shells or plates, have also been silicified. Silicification and dolomitization processes overlapped repeatedly, especially in the Jurassic rocks, being referred to as dolomitization interrupted by silicification (Radlicz, 1972). Calcitization of sponge spicules and crystallization of calcite at the expense of dolomite rhombohedral clusters were also observed. Pyritization is manifested by the presence of pyrite aggregates in bioclasts, and in spar and microspar calcite cements, or by the replacement of a part of rock with pyrite. The effect of replacement of calcite by anhydrite is also visible. Dedolomitization processes were also important in the rocks studied. Dolomitic limestones commonly appear to be composed of dolomite rhombohedra, at the expense of which large poikilotopic calcite crystals develop. Conditions allowing this process to take place occurred most likely after the buried sediment was elevated into the meteoric water zone. Dedolomitization was observed in a number of samples from the Miechów Trough (e.g., Kostki Małe 2 borehole, depths 1085.2 m and 1091.1m; Gidle 2 borehole, depths 1792.8 m and 1794.7 m). Among the neomorphic processes, micritization and sparitization of both the groundmass and granular components of carbonates are important. As a result of these processes, the texture of the rock was often blurred, and the grains became less visible, especially in peloidal limestones. This also resulted in the formation of micritic ooids and faunal debris, and of micrite coatings on skeletal grains. Kaolinite replaced partially or completely the original components of iron ooids, contributing to the development of intergranular porosity. Siderite replaced chamosite or bierthierine, and bioclasts and micas. Pyrite, calcite and apatite are locally found in glauconite aggregates.

The diagenetic dissolution process affected bioclasts, mainly aragonite bivalve shells, and ooids. Locally, their selective dissolution took place, leading to the formation of biomolds. Some of these were subsequently cemented with carbonates and kaolinite. Dissolution of halite, carbonates and anhydrite are also observed, and signs of etching of authigenic quartz are visible.

INTERPRETATION AND DISCUSSION

DIAGENETIC PROCESSES AND THEIR EFFECT ON FILTRATION PROPERTIES OF THE DEPOSITS

SILICICLASTIC ROCKS

Compaction, cementation and dissolution played the greatest role in creating the pore space of the sandstones.

Mechanical compaction, and much less so chemical compaction, are processes that significantly reduce the primary porosity of sedimentary rocks. However, precipitation of early overgrowth cements on grains (de Souza et al., 1995), particularly in the Lower Jurassic quartz arenites, was probably the factor that inhibited mechanical compaction.

Carbonate cementation has reduced the porosity of the sandstones. Early generation siderite crystallized in a temperature range of 15–40°C (Baker et al., 1995). Late-generation siderite in the Middle Jurassic sandstones crystallized under deep burial conditions at >55.0°C (Jarmołowicz-Szulc and Kozłowska, 2016). The formation of high-magnesium siderite may have been related to high concentrations of magnesium in the formation waters (Morad et al., 1994). According to Krystkiewicz (2008), dolomite crystallized after siderite at a temperature of about 75.6–79.0°C in the Lower Jurassic sandstones. Temperature studies of fluid inclusions in the late Mn-calcite cement of the Lower Triassic sandstones indicate that its crystallization temperatures generally did not exceed 100°C. Anhydrite cementation also reduces the sandstones' porosity.

Quartz cement such as overgrowths, if developed at an early stage, may have inhibited the action of mechanical compaction and contributed to the preservation of some of the primary porosity of the sandstones. The quartz, filling the pore space, has reduced it considerably. Studies of fluid inclusions in quartz cement of the Lower Jurassic sandstones of the Kuyavian region indicate its crystallization temperature in a range of 84.0–104.0°C (Krystkiewicz, 2008).

Crystallization of authigenic clay minerals in the pore space of a rock generally has a negative effect on its porosity. Early chlorites formed under reducing conditions presumably at temperatures ~20–40C (Grigsby, 2001). Kaolinite formed as a result of the action of meteoric water in an acidic environment (Bjørlykke, 1989). According to Osborn et al. (1994), vermiform kaolinite precipitates at 25–50°C. However, kaolinite can also increase the porosity because it forms at the expense of potassium feldspars or micas as these alter. This is because there is microporosity between the kaolinite crystals. The formation of kaolinite after micas may be explained by the co-occurrence of kaolinite and iron compounds in the pore space (Barczuk, 1979). The porosity and permeability of the sandstones were only slightly reduced by fibrous illite because of its local occurrence.

Diagenetic dissolution caused an increase in porosity. The effect of dissolution of grains and cements resulted in the formation of secondary porosity. Acidic meteoric waters, organic acids, and CO_2 released during the maturation of organic matter are the factors responsible for this process (Meshri, 1986; Crossey et al., 1986; Bjørlykke, 1989).

CARBONATE ROCKS

Compaction, cementation, replacement and dissolution are the most important processes forming the pore space in the carbonate rocks. Their primary porosity has been significantly reduced by mechanical and chemical compaction.

Cementation mainly by carbonates (calcite, dolomite, ankerite and siderite) and to a minor extent by anhydrite and siliceous cements generally deteriorates the reservoir properties of the rocks.

Replacement processes, mainly dolomitization, positively affect the filtration parameters of the rocks due to an increase in intracrystalline porosity. Pervasive dolomitization is related to fluid flow, resulting in localized mineralization with pyrite and sphalerite (Narkiewicz, 1983). During more intensive dolomitization, birdseye porosity or drusy fabric are produced (Welton, 1984). Silicification can help improve the reservoir

properties of the rocks. It was found that the silicified zones are both porous and permeable. Among the neomorphic processes, micritization may have improved the filtration capacity of the rocks, while aggradational neomorphism resulted in a reduction of porosity through grain growth and reduction of intergranular space.

Diagenetic dissolution, mainly of bioclasts, has led to an increase in porosity through the formation of secondary porosity.

RESERVOIR PROPERTIES

The results of the studies on diagenesis of Mesozoic strata in the Łódź and Miechów troughs, linked to the results of historical investigations, shed new light on the lithogenesis of the deposits and on the development of their reservoir characteristics.

Cementation and compaction are the diagenetic processes responsible for reducing primary porosity in the Lower Triassic sandstones, by ~21% and 50%, respectively (Fig. 9). Diagenetic dissolution and alteration have contributed to a localized increase in porosity in some sandstone beds. Traces of etching in cements and grains are particularly clearly visible in subarkosic arenites, which show increased porosity and permeability values. In general, the Buntsandstein section, excluding its lowermost and uppermost parts, is represented by rocks considered to be of relatively good reservoir properties. Their thickness is 20–380 m thick (Fijałkowska-Mader et al., 2015). Impermeable rocks are represented by mudstones, due to significant clay content. Permeability in the carbonate rocks is also close to zero because they are completely cemented and contain carbonate minerals recrystallized during diagenesis.

The Middle Triassic carbonate strata were subject to diagenetic processes shortly after deposition. Numerous allochems were bound by early calcite cements, often micritic, which prevented the sediment from blurring. With increasing burial, mechanical compaction increased, partly hampered by micrite rims on grains, and by the crystallization of later calcite cements in the form of spar. Diagenetic processes operating in the Muschelkalk rocks had both positive and negative effects on the development of porosity. The dissolution process, marked especially well in grainstones, was important for the formation of secondary porosity. Some of these rocks are characterized by very good reservoir properties and moderate filtration capacities. The thickness of these deposits is 40-250 m (Fijałkowska-Mader et al., 2015). However, in most of the carbonates the permeability is usually very low, even in porous levels, which confirms their poor reservoir properties.

The Upper Triassic siliciclastic rocks show low porosity (<10%) and their permeability is mostly low or zero. Such parameters are mainly due to mechanical compaction and cementation with quartz and carbonate minerals. Although microscopic studies have revealed the presence of secondary porosity due to dissolution of unstable components, much of the porosity has been reduced by cementation. Transformation of some of the components into fine-grained clay minerals, especially into chlorites, was also of great importance. The reasons for the lack of porosity in the carbonates are cementation by calcite, dolomite and, in places, anhydrite, as well as the recrystallization of micrite and microspar into spar. The Upper Triassic section is generally represented by non-reservoir rocks.

The Lower Jurassic sandstones show effects of the following diagenetic processes: compaction, cementation, dissolution, replacement and alteration. Compaction and cementation have reduced their primary porosity by about 45% and 35%, respectively (Fig. 9). Early overgrowth cements contributed to the preservation of some of the primary porosity in the rocks. Porosity was also reduced by carbonate cements, mainly siderite (a mineral of the siderite-magnesite isomorphic series) and ankerite. Primary porosity dominates, while secondary porosity (resulting from dissolution of grains and cements) and microporosity account for a small percentage. These sandstones show good and very good reservoir qualities. Their thickness is 20–90 m (Feldman-Olszewska, 2009).

After deposition, the Middle Jurassic rocks were bioturbated and subjected to mechanical compaction. Cementation with siderite or calcite, less frequently with dolomite, ankerite or authigenic quartz, also developed. The compaction and cementation have significantly reduced the porosity of the sandstones by ~55 and 35%, respectively (Fig. 9). Some sandstone beds have retained much of their intergranular primary porosity. Others are distinguished by low intergranular porosity, but they show secondary porosity due to dissolution of grains and decay of organic material. The Middle Jurassic sandstones can be classified into rocks of good reservoir properties as they show high porosities. Low-porosity rocks in the section include siltstones, claystones, limestones and siderites.

The dominant diagenetic process in the Upper Jurassic carbonate deposits was mechanical compaction that resulted in tighter packing of grains, often also grain deformation and fracturing. Among the processes that increased the porosity and permeability were micritization, dolomitization, silicification, and dissolution of calcium carbonate. The major processes that had a markedly negative effect on the filtration properties were sparitization, cementation by carbonates, anhydrite and pyrite, and dedolomitization. The Upper Jurassic deposits are porous to varying degrees, and show very poor permeability. Very good reservoir horizons include the cavernous and porous Oxfordian limestones. According to Jurkiewicz (1973), this is the result of karst developement.

The Lower Cretaceous rocks have undergone diagenetic processes, mainly compaction, cementation and dissolution. Due to mechanical and chemical compaction, the sandstones have reduced their primary porosity by an average of ~65%, while cementation processes have caused further decrease of ~15% (Fig. 9). Among the cements, quartz rims on detrital grains protected the pores from mechanical compaction, and led to the preservation of primary porosity. However, carbonate cementation had a negative effect on porosity. Dissolution processes, mainly of bioclasts and feldspars, have led to the development of secondary pores in the rocks. Some of the sandstones can be classified as reservoir rocks with good filtration properties. Their thickness depends on which formation the sandstones come from and varies from a few meters in the Bodzanowo Fm. to about 125 m in the Mogilno Fm. (Leszczyński, 2002). The limestones are represented by low-porosity and poorly permeable rocks.

The Upper Cretaceous rocks show effects of weak mechanical and chemical compaction due to dissolution under pressure. In the sandstones, the compaction has reduced their primary porosity by ~35% (Fig. 9). The cementation contributed to pore space reduction in the rocks. Due to precipitation of quartz and chalcedony cements, the primary porosity of the sandstones has decreased by up to 10% (Fig. 9). In the siliciclastic rocks, the preserved primary porosity is accompanied by secondary porosity that developed due to dissolution of detrital grains, mainly feldspar. In the carbonates, opal sponge spicules underwent dissolution. The porosity of carbonate-marly rocks in the Łódź Trough is high, but they are impermeable because their microporous structure. Most of the sandstones are porous and permeable. The quartz arenites and wackes found in the Upper Albian of the Łódź Trough, and in the Cenomanian and locally in the Maastrichtian of the Miechów Trough, show macroporosity and are classified as

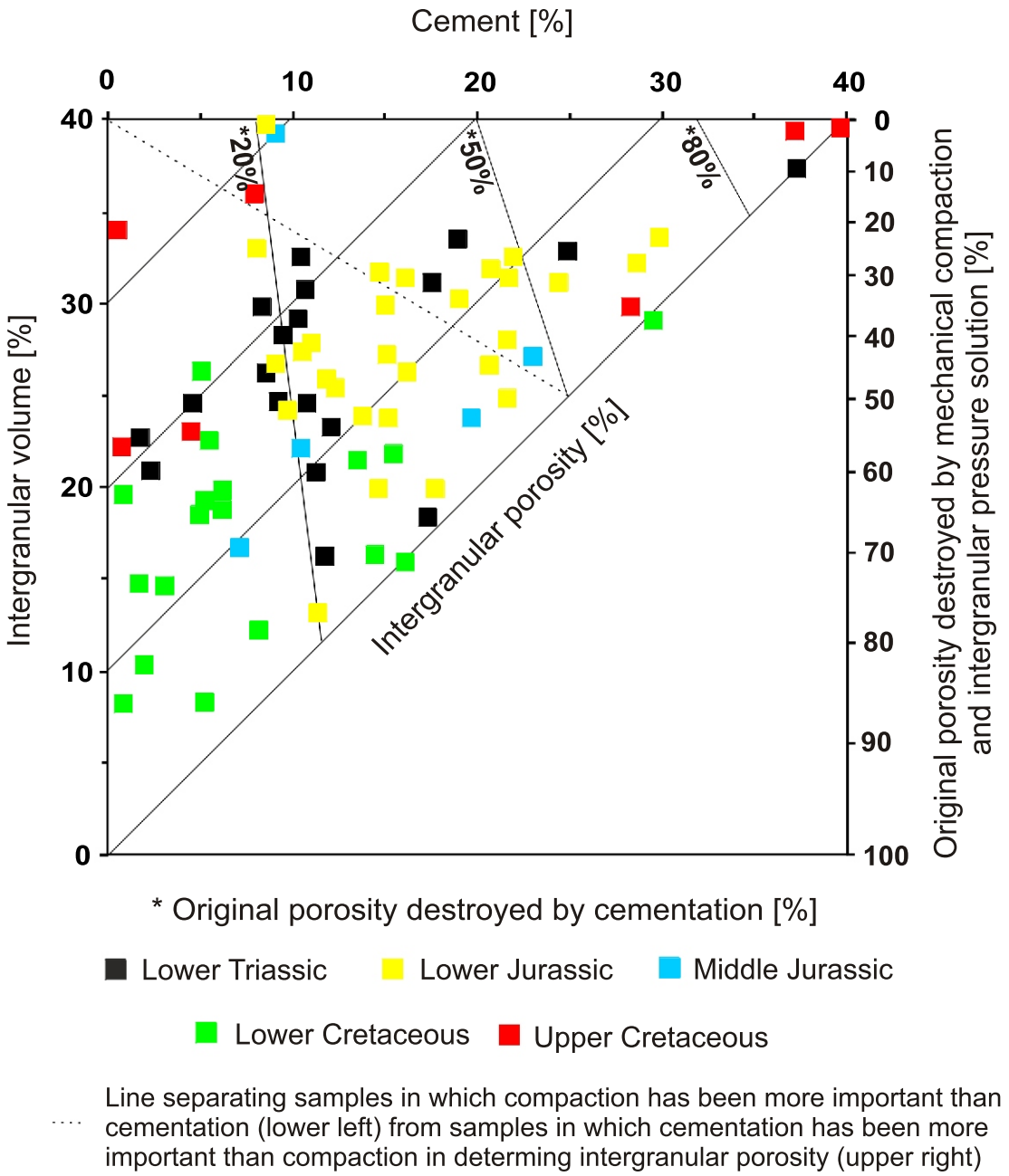

Fig. 9. Diagram modified from Houseknecht (1987) and Ehrenberg (1989) showing the effect of compaction and cementation on original porosity in the Triassic, Jurassic and Cretaceous sandstones

very good reservoir and filtration rocks. In contrast, the Santonian-Campanian calcareous quartz arenites of the Łódź Trough are characterized by poor porosity and show moderate filtration properties.

CONCLUSIONS

1. The Miechów Trough, by comparison with the Łódź Trough, is an area where rocks with better reservoir properties occur. Among these, sandstones are characterized by better filtration properties than carbonate rocks. The sandstones with the best reservoir properties are represented by arenites, mostly those of quartz and subarkosic types. Among the carbonate rocks, grainstones form the most prospective reservoir rock.

2. The most important diagenetic processes that influenced the pore space development of the sandstones are compaction, cementation and dissolution. Compaction and cementation have reduced their porosity by an average of ~44% and ~29%, respectively. These values are similar for the Miechów and Łódź troughs. The most intense compaction occurred in the Lower Cretaceous, Middle Jurassic and Lower Triassic sadstones (>50%). Cementation has reduced the porosity of the Lower Jurassic and Middle Jurassic sandstones to the greatest extent (~35%). Quartz, carbonates and clay minerals are the main cements that contributed to the porosity reduction. However, the formation of quartz cement in the form of overgrowths on quartz grains inhibited the effect of mechanical compaction and caused the preservation of a part of the primary porosity. Dissolution processes, mainly of feldspar grains, con-

tributed to the formation of secondary porosity in the sandstones and to the increase in porosity. This process was more intense during eodiagenesis than during mesodiagenesis.

3. Diagenetic processes of compaction, cementation, replacement and dissolution strongly affected the carbonate rocks. Eodiagenetic processes, such as compaction and cementation, negatively affected the development of pore space in the rocks. Mesodiagenetic processes, such as replacement processes, predominantly dolomitization, which increased intracrystalline porosity, had a positive effect on the porosity. The increase in the porosity took place also thanks to dissolution of bioclasts. In dolomitized grainstones with voids of dissolved grains, the porosity reaches ~24%. Chemical compaction is responsible for stylolitization processes which had a negative impact on the filtration properties of the rocks.

4. Sandstones of good reservoir properties are found in the Lower Triassic (Buntsandstein) and Lower Jurassic of the Miechów Trough and in the Lower Cretaceous of the Łódź Trough. The sandstones are characterized by a porosity of >15% (maximum 28%) and a permeability of >100 mD. Their thickness is 20–380 m in the Lower Triassic, and 20-90 m in the Lower Jurassic. In the Lower Cretaceous, their thickness varies from a few to about 125 m. Among the carbonates, those of the Middle Triassic (Muschelkalk) of the Miechów Trough show the best reservoir properties. The porosity of these rocks is commonly around 10%, with a maximum exceeding 26%. The porous (>10%) carbonate and carbonate-marly rocks, 40–250 m thick, are commonly impermeable.

Acknowledgements. The authors would like to thank the reviewers, Kinga Hips and two anonymous reviewers, for valuable and insightful comments and corrections have allowed improved our manuscript. The editor of Geological Quaterly, Prof. J. Rotnicka, is also warmly acknowledged for helpful suggestions. The authors would like to thank ORLEN Group for allowing them to use geological information owned by the company. The research was carried out at the Polish Geological Institute - National Research Institute and financed by the Ministry of Science and Higher Education (6.20.9143.00.0, 61.5205.0604.00.0, 62.9012.2325.00.0).

REFERENCES

Baker, J.C.J., Kassan, J., Hamilton, P.J., 1995. Early diagenetic siderite as indicator of depositional environment in the Triassic Rewan Group, Southern Bowen basin, eastern Australia. Sedimentology, **43**: 77–88; https://doi.org/10.1111/j.1365-3091.1996.tb01461.x

Bakker, R.J., Brown, P.E., 2003. Computer modeling in fluid inclusion research. Short Course. Mineral Association of Canada, **32**: 185–203; https://doi.org/10.3749/9780921294672.ch07

Barczuk, A., 1979. Petrographic study of the Buntsandstein sediments from the noth-eastern border of the Holy Cross Mts (Central Poland) (in Polish with English summary). Archiwum Mineralogiczne, **35**: 87–156.

Bjørlykke, K., 1989. Sedimentology and Petroleum Geology. Springer Verlag, Berlin.

Błaszkiewicz, A., Cieśliński, S., 1979. Works on systematization of stratigraphy of the Upper Cretaceous in Poland (except for the Carpathians and Sudety Mts) (in Polish with English summary). Kwartalnik Geologiczny, **23** (3): 639–648.

Bodnar, R.J., 1990. Petroleum migration in the Miocene Monterey Formation, California, USA: constraints from fluid inclusions studies. Mineralogical Magazine, **54**: 295–304; https://doi.org/10.1180/minmag.1990.054.375.15

Buła, Z., Habryn, R., 2010. Budowa geologiczna prekambru i paleozoiku region krakowskiego (in Polish). In: Prekambr i paleozoik regionu krakowskiego – model budowy geologicznej – jego aspekt utylitarny (eds. M. Jachowicz-Zdanowska and Z. Buła): 7–39. Konferencja naukowa Kraków, 19 listopada, 2010. Państwowy Instytut Geologiczny – Państwowy Instytut Badawczy.

Crossey, L.J., Surdam, R.C., Lahann, R., 1986. Application of organic/inorganic diagenesis to porosity prediction. SEPM Special Publication, **38**: 147–156; https://doi.org/10.2110/pec.86.38.0147

Dadlez, R., 1973. Szczegółowy profil litologiczno-stratygraficzny osadów retyku z otworu Strzelno IG 1 (in Polish). Profile Głębokich Otworów Wiertniczych Instytutu Geologicznego, **11**: 53–54.

Dadlez, R., 1997. Tektonika kompleksu permsko-mezozoicznego. Ogólne rysy tektoniczne bruzdy środkowopolskiej (in Polish). Prace Państwowego Instytutu Geologicznego, **153**: 410–414.

Dadlez, R., (ed.), 1998. Mapa tektoniczna kompleksu cechsztyńsko-mezozoicznego na Niżu Polskim, w skali 1 : 500 000 (in Polish with English summary). Państwowy Instytut Geologiczny, Warszawa.

Dadlez, R., Franczyk, M., 1976. Palaeogeographic and palaeotectonic significance of the Wielkopolska Ridge (Central Poland) in the Lower Jurassic Epoch (in Polish with English summary). Biuletyn Instytutu Geologicznego, **295**: 27–49.

Dadlez, R., Franczyk, M., 1977. Stratygrafia i paleogeografia. Retyk i jura dolna (in Polish). Prace Instytutu Geologicznego, **80**: 54–65.

Dayczak-Calikowska, K., 1977. Stratygrafia i paleogeografia. Jura środkowa. (in Polish). Prace Instytutu Geologicznego, **80**: 65–75.

Dayczak-Calikowska, K., Moryc, W., 1988. Evolution of sedimentary basin and palaeotectonics of the Middle Jurassic in Poland (in Polish with English summary). Kwartalnik Geologiczny, **32** (1): 117–136.

Dąbrowska, Z., 1970. The Upper Jurassic in the Mogilno-Łódź Depression (in Polish with English summary). Biuletyn Instytutu Geologicznego, **221**: 5–110.

Dąbrowska, Z., 1976. The Upper Jurassic of the Bełchatów Graben and Its Development in the other parts of the Łódź Trought (in Polish with English summary). Biuletyn Instytutu Geologicznego, **295**: 169–188.

Deczkowski, Z., 1997. Noryk i retyk. Wprowadzenie (in Polish). Prace Państwowego Instytutu. Geologicznego, **153**: 174–175.

Dembowska, J., 1973. Portlandian in the Polish Lowlands (in Polish with English summary). Prace Instytutu Geologicznego, **70**: 1–108.

Dembowska, J., 1977. Stratygrafia i paleogeografia. Jura górna (in Polish). Prace Instytutu Geologicznego, **80**: 75–83.

Dembowska, J., 1979. Systematization of lithostratigraphy of the Upper Jurassic in northern and central Poland (in Polish with English summary). Kwartalnik Geologiczny, **23** (3): 617–630.

De Souza, R.S., De Ros, L.F., Morad, S., 1995. Dolomite diagenesis and porosity preservation in lithic reservoirs: Carmópolis Member, Sergipe-Alagoas Basin, Northeastern Brazil. AAPG Bulletin, **79**: 725–748; https://doi.org/10.1306/8D2B1B88-171E-11D7-8645000102C1865D

Drits, V.A., 1997. Mixed-layer minerals. In: Modular aspects of minerals (ed. S. Merlino). 153–90; https://doi.org/10.1180/EMU-notes.1

Dunham, R., J., 1962. Classification of carbonate rocks according to depositional texture. AAPG Memoir, **1**: 108–121.

Ehrenberg, S.N., 1989. Assessing the relative importance of compaction processes and cementation to reduction of porosity in sadstones: discussion; compaction and porosity evolution of Pliocene sandstones, Ventura Basin, California: discussion. AAPG Bulletin, **73**: 1274–1276; https://doi.org/10.1306/44B4AA1E-170A-11D7-8645000102C1865D

Feldman-Olszewska, A., 1997a. Depositional systems and cyclicity in the intracratonic Early Jurassic basin in Poland. Geological Quarterly, **41** (4): 475–490.

Feldman-Olszewska, A., 1997b. Depositional architecture of the Polish epicontinental Middle Jurassic basin. Geological Quarterly, **41** (4): 491–508.

Feldman-Olszewska, A., 1998a. Hettangian – Late Toarcian Palaeogeography. In: Palaeogeographical Atlas of the Epicontinental Permian and Mesozoic in Poland 1:2 500 000 (eds. R. Dadlez, S. Marek and J. Pokorski). Plates 29–36. Warszawa.

Feldman-Olszewska, A., 1998b. Early Aalenian – Callovian Palaeogeography. In: Palaeogeographical Atlas of the Epicontinental Permian and Mesozoic in Poland 1 : 2 500 000 (eds. R. Dadlez, S. Marek and J. Pokorski). Plates 37–48. Warszawa.

Feldman-Olszewska, A., 2009. Wykonanie przestrzennych modeli facjalnych potencjalnych poziomów zbiornikowych i poziomów ekranujących. Korelacje międzyotworowe (in Polish). In: Rozpoznanie formacji i struktur do bezpiecznego geologicznego składowania CO_2 wraz z ich programem monitorowania, Raport merytoryczny nr 2: Segment I, rejon Bełchatów: 25–47; https://skladowanie.pgi.gov.pl/twiki/pub/CO2/WynikiBelchatow/Segment_I%2c_Be%b3chat%f3w.pdf

Feldman-Olszewska, A., 2012a. Stratygrafia i litologia utworów jury dolnej na tle rozwoju paleotektonicznego strefy Ponętów-Wartkowice (in Polish). Profile Głębokich Otworów Wiertniczych Państwowego Instytutu Geologicznego, **133**: 84–87.

Feldman-Olszewska, A., 2012b. Stratygrafia i litologia utworów jury środkowej na tle rozwoju paleotektonicznego strefy Ponętów-Wartkowice (in Polish). Profile Głębokich Otworów Wiertniczych Państwowego Instytutu Geologicznego, **133**: 94–96.

Fijałkowska-Mader, A., Kuleta, M., Zbroja, S., 2015. Lithostratigraphy, palynofacies and depositional environments of the Triassic deposits in the northern part of the Nida Basin (in Polish with English summary). Biuletyn Państwowego Instytutu Geologicznego, **462**: 83–124; https://doi.org/10.5604/08676143.1157486

Folk, R.L., 1959. Practical petrographic classification of limestones. AAPG Bulletin, **43**: 1–38; http://pubs.geoscienceworld.org/aapgbull/article-pdf/43/1/1/4379722/aapg_1959_0043_0001_0001.pdf

Gajewska, I., 1977. Stratygrafia i paleogeografia. Wapień muszlowy i kajper (in Polish). Prace Instytutu Geologicznego, **80**: 50–53.

Gajewska, I., 1978. The stratigraphy and development of the Keuper in north-west Poland (in Polish with English summary). Prace Instytutu Geologicznego, **87**: 5–59.

Gajewska, I., 1988a. Palaeothickness and lithofacies of the Muschelkalk and Lower Keuper and the Middle Triassic palaeotectonics in Polish Lowland (in Polish with English summary). Kwartalnik Geologiczny, **32** (1): 73–82.

Gajewska, I., 1988b. Palaeothickness, lithofacies and palaeotectonics the Upper Keuper in Polish Lowland (in Polish with English summary). Kwartalnik Geologiczny, **32** (1): 83–92.

Gajewska, I., 1997. Trias górny. Kajper. Sedymentacja, paleogeografia i paleotektonika (in Polish). Prace Państwowego Instytutu Geologicznego, **153**: 166–172.

Goldstein, R.H., Reynolds, T.J., 1994. Systematics of fluid inclusions in diagenetic minerals. SEPM Short Course, **31**: 199; https://doi.org/10.2110/scn.94.31

Grigsby, J.D., 2001. Origin and growth mechanism of authigenic chlorite in sandstones of the Lower Vickburg Formation, South Texas. Journal of Sedimentary Research, **71**: 27–36; http://pubs.geoscienceworld.org/sepm/jsedres/article-pdf/71/1/27/2814454/27.pdf

Hakenberg, M., 1986. Albian and Cenomanian in the Miechów Basin (Central Poland) (in Polish with English summary). Studia Geologica Polonica, **136**: 57–85.

Hakenberg, M., Jurkiewicz, H., Woiński J., 1973. Profiles of Middle Cretaceous in the northern part of the Miechów Trough (in Polish with English summary). Kwartalnik Geologiczny, **17** (4): 763–786.

Harris, P.M., Kendal, G., Lerche, J., 1985. Carbonate cementation – a brief review. SEPM Special Publication, **36**: 79–95; https://doi.org/10.2110/pec.85.36.0079

Horton, D.G., 1985. Mixed-layer illite/smectite as a paleotempereature indicator in Amethyst vein system, Creede district, Colorado, USA. Contributions to Mineralogy and Petrology, **91**: 171–179; https://doi.org/10.1007/BF00377764

Houseknecht, D.W., 1987. Assessing the relative importance of compaction processes and cementation to reduction of porosity in sandstones. AAPG Bulletin, **71**: 633–642; https://doi.org/10.1306/9488787F-1704-11D7-8645000102C1865D

Jarmołowicz-Szulc, K., Kozłowska, A., 2016. Temperature and isotopic relations in carbonate minerals in the Middle Jurassic sideritic rocks of central and southern Poland. Geological Quarterly, **60** (4): 881–892; https://doi.org/10.7306/gq.1323

Jaskowiak-Schoeneichowa, M., Krassowska, A., 1988. Palaeothickness, lithofacies and palaeotectonics of the epicontinental Upper Cretaceous in Poland (in Polish with English summary). Kwartalnik Geologiczny, **32** (1): 177–198.

Jaworowski, K., 1987. Petrographic canon of the most common sedimentary rocks (in Polish). Przegląd Geologiczny, **35**: 205–209.

Jurkiewicz, H., 1965. Structure of the Nida trough in the margin of the Święty Krzyż Mts and possibilities of oil and gas occurrences (in Polish with English summary). Przegląd Geologiczny, **13**: 339–342.

Jurkiewicz, H., 1973. Development of the Triassic in the central area of the Nida Trough (in Polish with English summary). Kwartalnik Geologiczny, **18** (1): 90–109.

Jurkiewicz, H., (ed.), 1974a. Węgleszyn IG 1 (in Polish). Profile Głębokich Otworów Wiertniczych Instytutu Geologicznego, **19**.

Jurkiewicz, H., (ed.), 1974b. Milianów IG 1 (in Polish). Profile Głębokich Otworów Wiertniczych Instytutu Geologicznego, **21**.

Jurkiewicz, H., (ed.), 1976a. Pągów IG 1 (in Polish). Profile Głębokich Otworów Wiertniczych Instytutu Geologicznego, **33**.

Jurkiewicz, H., (ed.), 1976b. Jarowice IG 1 (in Polish). Profile Głębokich Otworów Wiertniczych Instytutu Geologicznego, **34**.

Jurkiewicz, H., (ed.), 1994. Secemin IG 1 (in Polish). Profile Głębokich Otworów Wiertniczych Instytutu Geologicznego, **77**.

Jurkowska, A., 2016. Inoceramid stratigraphy and depositional architecture of the Miechów Synclinorium (southern Poland). Acta Geologica Polonica, 66: 59–84; https://doi.org/10.1515/agp-2015-0025

Jurkowska, A., Świerczewska-Gładysz, E., 2022. Opoka – a mysterious carbonate-siliceous rock: an overview of general concepts. Geology, Geophysics & Environment, **48**: 257–278; https://doi.org/10.7494/geol.2022.48.3.257

Karnkowski, P., 1993. Złoża gazu ziemnego i ropy naftowej w Polsce. Niż Polski (in Polish). **1**. Wyd. GEOS, AGH, Kraków.

Kopik, J., 1979. Stratigraphy of the Middle Jurassic of the Bełchtów region (in Polish with English summary). Kwartalnik Geologiczny, **23** (1): 179–194.

Kozłowska, A., Krystkiewicz, E., 2012. Wyniki badań petrograficznych utworów jury dolnej (in Polish). Profile Głębokich Otworów Wiertniczych Państwowego Instytutu Geologicznego, **135**: 87–94.

Kozłowska, A., Kuberska, M., 2014. Diagenesis and porosity of the Lower Jurassic sandstones in the Polish Lowlands (in Polish with English summary). Biuletyn Państwowego Instytutu Geologicznego, **458**: 39–60.

Kozłowska, A., Kuberska, M., Pańczyk, M., Sikorska, M., 2010. Pore space in Lower Jurassic sandstones of the Bełchatów region (in Polish with English summary). Biuletyn Państwowego Instytutu Geologicznego, **439**: 37–46.

Kozłowska A., Kuberska M., Krystkiewicz E., 2012. Wyniki badań petrograficznych utworów jury dolnej (in Polish). Profile Głębokich Otworów Wiertniczych Państwowego Instytutu Geologicznego, **137**: 126–138.

Kozłowska, A., Feldman-Olszewska, A., Kuberska, M., Maliszewska, A., 2021. Diagenesis and the conditions of deposition of the Middle Jurassic siderite rocks from the northern margin of the Holy Cross Mountains (Poland). Minerals, **11**, 1353; https://doi.org/10.3390/min11121353

Krassowska, A., 1997. Formalne i nieformalne jednostki litostratygraficzne. Kreda górna (in Polish). Prace Państwowego Instytutu Geologicznego, **153**: 382–383.

Krystkiewicz, E., 1999a. Upper Triassic – Keuper, Norian, Rhaetian (in Polish with English summary). Prace Państwowego Instytutu Geologicznego, **167**: 51–63.

Krystkiewicz, E., 1999b. Lower Jurassic (in Polish with English summary). Prace Państwowego Instytutu Geologicznego, **167**: 64–77.

Krystkiewicz E., 2008. Wyniki badań petrograficznych utworów jury dolnej. Profile Głębokich Otworów Wiertniczych Państwowego Instytutu Geologicznego, **125**: 141–149.

Krzywiec, P., 2006. Structural inversion of the Pomeranian and Kuiavian segments of the Mid-Polish Trough – lateral variations in timing and structural style. Geological Quarterly, **50** (1): 151–168.

Krzywiec, P., Gutowski, J., Walaszczyk, I., Wróbel, G. Wybraniec, S., 2009. Tectonostratigraphic model of the Late Cretaceous inversion along the Nowe Miasto–Zawichost Fault Zone, SE Mid-Polish Trough. Geological Quarterly, **53** (1): 27–48.

Kuberska, M., 1997. The Lower Triassic (in Polish with English summary). Prace Państwowego Instytutu Geologicznego, **153**: 117–121.

Kuberska, M., 1999. Lower Triassic – Buntsandstein (in Polish with English summary). Prace Państwowego Instytutu Geologicznego, **167**: 22–35.

Kuberska, M., Becker A., Kozłowska, A., 2019. The characteristics of pore space in Lower Triassic sandstones of the Warsaw region. Biuletyn Państwowego Instytutu Geologicznego, **474**: 73–84; https://doi.org/10.5604/01.3001.0013.0826

Kuberska, M., Kozłowska, A., Wołkowicz, K., 2023. Triassic and Jurassic siliciclastic rocks of the Łódź-Miechów Syncline in the aspect of the development of their pore space (in Polish with English summary). Przegląd Geologiczny, **71**: 212–218; https://doi.org/10.7306/2023.16

Leszczyński, K., 2000. The Late Cretaceous sedimentation and subsidence south-west of the Kłodawa Salt Diapir, central Poland. Geological Quarterly, **44** (2): 167–174.

Leszczyński, K., 2002. The Cretaceous evolution of the Ponętów-Wartkowice zone (in Polish with English summary). Prace Państwowego Instytutu Geologicznego, **176**.

Leszczyński, K., 2010. Lithofacies evolution of the Late Cretaceous basin in the Polish Lowlands (in Polish with English summary). Biuletyn Państwowego Instytutu Geologicznego, **443**: 33–54.

Maliszewska, A., 1971. Osady psefitowe doggeru z niecki mogileńsko-łódzkiej. Opracowanie osadów psefitowych doggeru z wierceń Strzelno IG 1 i Madaje Stare IG 1 oraz osadów keloweju i Oksfordu z wiercenia Osowa (in Polish). Inw. 134103. NAG, Państwowy Instytut Geologiczny – Państwowy Instytut Badawczy, Warszawa.

Maliszewska, A., 1972. The origin of Lisów Breccia on the basis of petrographic studies (in Polish with English summary). Biuletyn Instytutu Geologicznego, **261**: 33–54.

Maliszewska, A., 1998. New petrological data on carbonate mineralogy in the Middle Jurassic siliciclastic deposits of the Kujawy region (Polish Lowlands). Geological Quarterly, **42** (4): 401–420.

Maliszewska, A., (ed.), 1999. Diagenesis of the Upper Permian and Mesozoic deposits of the Kujawy region (Central Poland) (in Polish with English summary). Prace Państwowego Instytutu Geologicznego, **167**.

Marek, S., 1977a. Sytuacja geotektoniczna (in Polish). Prace Instytutu Geologicznego, **80**: 7–11.

Marek, S., 1977b. Stratygrafia i paleogeografia. Kreda dolna. (in Polish). Prace Instytutu Geologicznego, **80**: 83–99.

Marek, S., 1997. Formalne i nieformalne jednostki litostratygraficzne. Kreda dolna (berias – alb górny) (in Polish). Prace Państwowego Instytutu Geologicznego, **153**: 351–360.

Marek, S., Raczyńska, A., 1979. Lithostratigraphic subdivision of epicontinental Lower Cretaceous in Poland and proposals for its rearrangement (in Polish with English summary). Kwartalnik Geologiczny, **23** (3): 631–637.

Marek, S., Rajska, M., Sztejn, J., 1989. New views on stratigraphy of the Jurassic-Cretaceous boundary in central Poland (Kujawy) (in Polish with English summary). Kwartalnik Geologiczny, **33** (2): 209–224.

Meshri, I.D., 1986. On the reactivity of carbonic and organic acids and generation of secondary porosity. SEPM Special Publication, **38**: 123–128; https://doi.org/10.2110/pec.86.38.0123

Migaszewski, Z., Narkiewicz, M., 1983. Identification of common carbonate minerals with the use of colouring indices (in Polish with English summary). Przegląd Geologiczny, **31**: 258–261.

Morad, S., Ben, Ismail, H.N., De Ros, L.F., Al-Aasm, I.S., Sherrhini, N.E., 1994. Diagenesis and formation water chemistry of Triassic reservoir sandstones from Southern Tunisia. Sedimentology, **41**: 1253–1272; https://doi.org/10.1111/j.1365-3091.1994.tb01452.x

Mrozek, K., 1975. Budowa geologiczna struktur wgłębnych w południowej części synklinorium łódzkiego (in Polish). Wydaw. Geol., Warszawa.

Narkiewicz, M., 1983. The dolomite puzzle (in Polish with English summary). Przegląd Geologiczny. **31**: 37–42.

Narkiewicz, K., Szulc, J., 2004. Controls on migration of conodont fauna in peripherial oceanic areas. An example from the Middle Triassic of the Northern Peri-Tethys. Geobios, **37**: 425–436; https://doi.org/10.1016/j.geobios.2003.10.001

Narkiewicz, M., Dadlez, R., 2008. Geological regional subdivision of Poland: general guidelines and proposed schemes of sub-Cenozoic and sub-Permian units (in Polish with English summary). Przegląd Geologiczny, **56**: 391–397.

Niemczycka, T., 1997. Jura górna (in Polish). Prace Państwowego Instytutu Geologicznego, **153**: 309–322.

Nowicka, M., 1973. Kajper. Wyniki badań petrograficznych (in Polish). Profile Głębokich Otworów Wiertniczych Instytutu Geologicznego, **5**: 95–109.

Osborne, M., Haszeldine, R.S., Fallick, A.E., 1994. Variation in kaolinite morphology with growth temperature in isotopically mixed pore-fluids, Brent Group, UK North Sea. Clay Minerals, **29**: 591–608; https://doi.org/10.1180/claymin.1994.029.4.15

Pettijohn, F.J., Potter, P.E., Siever, R., 1972. Sand and Sandstones. Springer Verlag, New York.

Pieńkowski G., 2004. The epicontinental Lower Jurassic of Poland. Polish Geological Institute Special Papers, **12**.

Połońska, M., 1999a. Lower Cretaceous (in Polish with English summary). Prace Państwowego Instytutu Geologicznego, **167**: 112–127.

Połońska, M., 1999b. Upper Cretaceous (in Polish with English summary). Prace Państwowego Instytutu Geologicznego, **167**: 128–138.

Połońska, M., 2000. Microlithofacies variability of Lower Cretaceous deposits in the western part of the Płock Trough. Prace Specjalne PTM, **17**: 233–234.

Połońska, M., 2007. Ferruginous ooids as an indicator for the evolution of the Cretaceous deposits between Toruń and Warsaw (in Polish with English summary). Przegląd Geologiczny, **55**: 302–303.

Połońska, M., 2010. Petrology and diagenesis of the Lower Cretaceous sandstones from the Płock Trough (in Polish with English summary). Biuletyn Państwowego Instytutu Geologicznego, **443**: 55–80.

Połońska, M., Wołkowicz, K., 2005. Osady najmłodszej jury i najstarszej kredy Polski centralnej i północno-zachodniej w świetle badań petrologicznych (in Polish). Volumina Jurassica, **3**: 144–145.

Pożaryski, W., 1969. Division of the area of Poland into tectonic units (in Polish with English summary). Przegląd Geologiczny, **17**: 57–64.

Radlicz, K., 1966. The structures of stylolites (in Polish with English summary). Kwartalnik Geologiczny, **10** (2): 367–382.

Radlicz, K., 1972. Lithology of the Upper Jurassic deposits in north-eastern Poland (in Polish with English summary). Biuletyn Instytutu Geologicznego, **261**: 55–169.

Radlicz, K., 1999. Jura górna. Wpływ procesów diagenetycznych na fizyczne cechy osadów (in Polish). Prace Państwowego Instytutu Geologicznego, **167**: 94–111.

Raczyńska, A., 1973. Wyniki badań stratygraficznych i litologicznych. Kreda dolna (in Polish). Profile Głębokich Otworów Wiertniczych Instytutu Geologicznego, **11**: 80–88.

Raczyńska, A., 1979. The stratigraphy and lithofacies development of the younger Lower Cretaceous in the Polish Lowlands (in Polish with English summary). Prace Instytutu Geologicznego, **89**.

Rutkowski, J., 1965. Senonian in the area of Miechów, Southern Poland (in Polish with English summary). Rocznik Polskiego Towarzystwa Geologicznego, **35**: 3–46.

Ryka, W., Maliszewska, A., 1991. Słownik petrograficzny (in Polish). 2nd edition. Wydaw. Geol., Warszawa.

Ryll, A., 1973. Szczegółowy profil litologiczno-petrograficzny osadów jury środkowej z otworu Strzelno IG 1 (in Polish). Profile Głębokich Otworów Wiertniczych Instytutu Geologicznego, **11**: 44–53.

Senkowiczowa, H., 1979. On possibilities to formalize lithostratigrapidc subdivision of the epicontinental Middle and Upper Triassic of Poland (in Polish with English summary). Kwartalnik Geologiczny, **23** (3): 583–600.

Sikorska, M., 1994. Cathodoluminescence: an essential tool in diagenetic studies of Cambrian sandstones of northern and eastern Poland (in Polish with English summary). Przegląd Geologiczny, **52**: 256–263.

Szyperko-Śliwczyńska, A., 1977. Stratygrafia i paleogeografia. Piaskowiec pstry dolny i środkowy (inPolish). Prace Instytutu Geologicznego, **80**: 39–48.

Szyperko-Śliwczyńska, A., 1979. Lower Trias in north-eastern Poland (in Polish with English summary). Prace Instytutu Geologicznego, **91**: 1–77.

Szyperko-Śliwczyńska, A., 1980. Lithostratigraphy of the Bundsandstein of Poland and project of its systematization (in Polish with English summary). Kwartalnik Geologiczny, **24** (2): 275–298.

Szyperko-Teller, A., 1982. Lithostratigraphy of the Buntsandstein in the Western Pomerania (in Polish with English summary). Kwartalnik Geologiczny, **26** (2): 341–368.

Szyperko-Teller, A., 1997. Trias dolny. Litostratygrafia i litofacje. Formalne i nieformalne jednostki litostratugraficzne (in Polish). Prace Państwowego Instytutu. Geologicznego **153**: 112–117.

Szyperko-Teller, A., Moryc, W., 1988. Evolution of the Buntsandstein sedimentary basin in Poland (in Polish with English summary). Kwartalnik Geologiczny, **32** (1): 53–72.

Świerczewska-Gładysz, E. 2016. Early Campanian (Late Cretaceous) Pleromidae and Isoraphiniidae (lithistid Demospongiae) from the Łódź-Miechów Synclinorium (central and southern Poland): new data and taxonomic revision. Palaeontology, **2**: 189–233; https://doi.org/10.1002/spp2.1037

Świerczewska-Gładysz, E., Jurkowska, A., 2023. Taxonomy and palaeoecology of the Late Cretaceous (Campanian) phymatellidae (lithistid demosponges) from the Miechów and Mogilno-Łódź Synclinoria (southern and central Poland). Annales Societatis Geologorum Poloniae, **93**: 269–304; https://doi.org/10.14241/asgp.2023.03

Welton, J.E., 1984. SEM Petrology Atlas. American Association of Petroleum Geologists.

Wołkowicz, K., 1999. Middle Trissic – Muschelkalk (in Polish with English summary). Prace Państwowego Instytutu Geologicznego, **167**: 36–51.

Złonkiewicz, Z., 2006. Evolution of the Miechów Depresion basin in the Jurassic as a result of regional tectonical changes (in Polish with English summary). Przegląd Geologiczny, **54**: 534–540.

Złonkiewicz, Z., 2009. The Callovian and Upper Jurassic section in the Nida Through (in Polish with English summary). Przegląd Geologiczny, **57**: 521–530.

APPENDIX 1

Statistical results of computer image analysis of pore space and porosity of selected sandstone samples

Borehole	Eq Diameter	Perimeter	Mean Chord	Length	Width	Max Feret	Min Feret	Circularity	Elongation	Porosity
Depth	[mm]	[mm]	[mm]	[mm]	[mm]	[mm]	[mm]	[mm]	[mm]	[%]
SANDSTONES OF THE LOWER TRASSIC										
	0.0035565	0.020541	0.0025869	0.0094401	0.0020478	0.0048557	0.0030745	0.97849	1.4113	
Brzegi IG 1	0.011943	0.24039	0.027762	0.11925	0.00192	0.024606	0.014319	0.096845	0.62121	14.65
1529.3 m	0.0020424	0.0048535	0.0021205	0.00181	0.0014994	0.00181	0.00181	0.0081873	1	
	0.30383	10.272	0.051611	5.122	0.036237	0.66111	0.47747	1	4	
	0.0029734	0.011736	0.0024335	0.0051506	0.0019396	0.0037241	0.0023726	0.98254	1.4147	
Brzegi IG 1	0.0083885	0.096674	0.0020935	0.047157	0.0014251	0.017827	0.0077542	0.078873	0.64073	11.99
1558.4 m	0.0020424	0.0048535	0.0021205	0.00181	0.0014994	0.00181	0.00181	0.026638	1	
	0.40639	5.3214	0.076577	2.611	0.049678	0.9925	0.38397	1	6	
	0.0026992	0.0092071	0.00235	0.00396	0.00187	0.00318	0.00209	0.98428	1.46400	
Pągów IG 1	0.0041751	0.06088	0.00091	0.02999	0.00060	0.00833	0.00429	0.06749	0.64432	10.12
2330.5 m	0.0020424	0.00485	0.00212	0.00181	0.00150	0.00181	0.00181	0.022234	1	
	0.16756	3.39610	0.03444	1.68600	0.02484	0.43791	0.19005	1	5	
	0.00278	0.01307	0.00235	0.00587	0.00189	0.00335	0.00229	0.98494	1.38890	
Pągów IG 1	0.00733	0.20471	0.00101	0.10195	0.00067	0.01562	0.00927	0.06805	0.61351	10.05
2362.7 m	0.00204	0.00485	0.00212	0.00181	0.00150	0.00181	0.00181	0.0071616	1	
	0.44527	16.53000	0.03403	8.24610	0.02559	0.98068	0.67040	1	9	
	0.00276	0.00973	0.00238	0.00417	0.00191	0.00335	0.00222	0.98105	1.39260	
Secemin IG 1	0.00548	0.07555	0.00120	0.03714	0.00081	0.01517	0.00543	0.08135	0.61370	6.41

1990.8 m	0.00204	0.00485	0.00212	0.00181	0.00150	0.00181	0.00181	0.027055	1	
	0.31002	5.29400	0.07075	2.62400	0.04632	0.99878	0.32716	1	8	
	0.00275	0.00982	0.00237	0.00423	0.00189	0.00324	0.00217	0.98173	1.40630	
Secemin IG 1	0.00623	0.10555	0.00125	0.05219	0.00084	0.01165	0.00611	0.08034	0.63755	11.26
2003.6 m	0.00204	0.00485	0.00212	0.00181	0.00150	0.00181	0.00181	0.02466	1	
	0.46058	9.21430	0.05680	4.57070	0.03645	0.74779	0.47844	1	7	
CARBONATES OF THE MIDDLE TRIASSIC										
	0.00277	0.01067	0.00238	0.00470	0.00188	0.00328	0.00209	0.98392	1.54560	
Gidle 2	0.00598	0.13571	0.00151	0.06744	0.00102	0.00951	0.00562	0.05341	0.68057	23.43
1788.3 m	0.00204	0.00485	0.00212	0.00181	0.00150	0.00181	0.00181	0.00321	1	
	0.39562	14.07700	0.10825	7.02100	0.07705	0.63356	0.34033	1	6	
	0.00259	0.00768	0.00233	0.00325	0.00183	0.00298	0.00191	0.98668	1.5517	
Gidle 2	0.00189	0.03404	0.00040	0.01687	0.00025	0.00371	0.00210	0.04908	0.66477	10.19
1790.0 m	0.00204	0.00485	0.00212	0.00181	0.00150	0.00181	0.00181	0.01240	1	
	0.15144	3.86570	0.02428	1.92350	0.01567	0.29218	0.21927	1	9	
	0.00249	0.00697	0.00229	0.00288	0.00183	0.00275	0.00190	0.98731	1.4429	
Radziątków 7	0.00194	0.01677	0.00062	0.00804	0.00041	0.00305	0.00187	0.04470	0.65507	6.33
2560.0 m	0.00204	0.00485	0.00212	0.00181	0.00150	0.00181	0.00181	0.04118	1	
	0.13271	1.0019	0.045724	0.49429	0.031151	0.17871	0.12851	1	4	
SANDSTONES OF THE UPPER TRIASSIC										
	0.00263	0.00869	0.00233	0.00370	0.00187	0.00303	0.00209	0.98333	1.41630	
Gidle 2	0.00312	0.05661	0.00066	0.02804	0.00044	0.00657	0.00376	0.06974	0.63054	10.81
1618.6 m	0.00204	0.00485	0.00212	0.00181	0.00150	0.00181	0.00181	0.00717	1	
	0.16368	6.07450	0.02243	3.03030	0.01469	0.43764	0.23979	1	8.6515	

	0.00308	0.01350	0.00250	0.00600	0.00198	0.00378	0.00249	0.97716	1.46460	
Secemin IG 1	0.00710	0.21003	0.00141	0.10464	0.00099	0.01293	0.00763	0.09038	0.63693	13.78
1414.6 m	0.00204	0.00485	0.00212	0.00181	0.00150	0.00181	0.00181	0.00549	1	
	0.47478	20.12600	0.03183	10.04500	0.02137	0.89839	0.49624	1	6	
	0.00264	0.00761	0.00238	0.00313	0.00191	0.00300	0.00206	0.98391	1.42780	
Węgleszyn IG1	0.00217	0.01444	0.00085	0.00669	0.00061	0.00402	0.00183	0.05742	0.61236	1.55
2013.6 m	0.00204	0.00485	0.00212	0.00181	0.00150	0.00181	0.00181	0.07568	1	
	0.08438	0.52847	0.03325	0.24103	0.02320	0.16288	0.05538	1	3	
SANDSTONES OF LOWER JURASSIC										
Banachów IG 1	0.00265	0.00846	0.00235	0.00360	0.00186	0.00308	0.00203	0.98488	1.4951	
3338.2	0.00441	0.05221	0.00132	0.02551	0.00096	0.00792	0.00454	0.05508	0.68594	7.00
	0.00204	0.00485	0.00212	0.00181	0.00150	0.00181	0.00181	0.01768	1	
	0.25259	2.90010	0.06561	1.44180	0.05227	0.41868	0.24616	1	4.2049	
Kłokoczyn 1	0.00320	0.01336	0.00251	0.00592	0.00198	0.00413	0.00268	0.97825	1.4543	
1049.1	0.00824	0.08909	0.00217	0.04330	0.00149	0.01632	0.00979	0.09160	0.67618	13.2
	0.00204	0.00485	0.00212	0.00181	0.00150	0.00181	0.00181	0.04922	1	
	0.2208	2.9688	0.042424	1.4581	0.032593	0.44422	0.28477	1	6	
	0.00284	0.01013	0.00240	0.00438	0.00191	0.00340	0.00225	0.98065	1.4446	
Pągów IG 1	0.00508	0.06545	0.00131	0.03209	0.00089	0.00962	0.00526	0.07980	0.65737	13.3
1526.0	0.00204	0.00485	0.00212	0.00181	0.00150	0.00181	0.00181	0.02564	1	
	0.2169	3.8773	0.0326	1.9194	0.0216	0.42508	0.22037	1	6	
	0.00407	0.02275	0.00275	0.01043	0.00216	0.00591	0.00358	0.97032	1.4405	
Ponętów 2	0.01342	0.16800	0.00344	0.08226	0.00235	0.02781	0.01564	0.12063	0.66632	14.7
2633.2	0.00204	0.00485	0.00212	0.00181	0.00150	0.00181	0.00181	0.01251	1	

	0.25916	4.4568	0.064668	2.2068	0.04428	0.58255	0.3757	1	7	
	0.00318	0.01290	0.00251	0.00571	0.00198	0.00407	0.00255	0.97598	1.5255	
Secemin IG 1	0.00810	0.09158	0.00213	0.04463	0.00146	0.01566	0.00880	0.08671	0.71102	13.2
1374.5	0.00204	0.00485	0.00212	0.00181	0.00150	0.00181	0.00181	0.02545	1	
	0.22187	3.7854	0.059382	1.8772	0.041903	0.49694	0.25193	1	6	
	0.0026257	0.0078683	0.0023495	0.0032906	0.0018746	0.003038	0.0020243	0.98307	1.4551	
Zgierz IG 1	0.0024746	0.020688	0.00082462	0.0098645	0.0005839	0.0050505	0.0023263	0.06565	0.66557	4.7
2405.0-2407.0	0.0020424	0.0048535	0.0021205	0.00181	0.0014994	0.00181	0.00181	0.043643	1	
	0.089492	0.77595	0.025467	0.37102	0.016953	0.17154	0.078151	1	5	
SANDSTONES OF THE MIDDLE JURASSIC										
	0.00521	0.06242	0.00274	0.03028	0.00214	0.00886	0.00535	0.97071	1.43390	
Poddębice IG 2	0.02812	0.81641	0.00384	0.40670	0.00256	0.06406	0.04001	0.12696	0.67346	27.19
3189.0 m	0.00204	0.00485	0.00212	0.00181	0.00150	0.00181	0.00181	0.00304	1	
	0.69560	27.35600	0.10152	13.65000	0.06600	1.45890	0.99188	1	14	
	0.00380	0.01861	0.00273	0.00834	0.00217	0.00529	0.00322	0.97469	1.36040	
Ponętów 2	0.01322	0.14641	0.00438	0.07124	0.00311	0.02691	0.01249	0.10611	0.58962	11.38
2431.5 m	0.00204	0.00485	0.00212	0.00181	0.00150	0.00181	0.00181	0.01542	1	
	0.31088	5.19690	0.14241	2.58560	0.10344	0.63574	0.23652	1	6	
	0.00416	0.02976	0.00267	0.01396	0.00211	0.00622	0.00378	0.96741	1.35790	
Żerechowa 2	0.01466	0.30701	0.00257	0.15241	0.00172	0.03285	0.01683	0.13419	0.59482	22.07
1293.8 m	0.00204	0.00485	0.00212	0.00181	0.00150	0.00181	0.00181	0.00963	1	
	0.54304	17.38900	0.04910	8.66750	0.03196	1.21890	0.64558	1	5	
CARBONATES OF THE UPPER JURASSIC										
	0.00248	0.00675	0.00230	0.00278	0.00183	0.00276	0.00186	0.98904	1.4806	

Węgleszyn IG 1	0.00073	0.00575	0.00027	0.00282	0.00015	0.00166	0.00058	0.03745	0.64554	1.59
1023.6 m	0.00204	0.00485	0.00212	0.00181	0.00150	0.00181	0.00181	0.06096	1	
	0.036191	0.45671	0.0084911	0.22376	0.0066132	0.11346	0.047958	1	6	
SANDSTONES OF THE LOWER CRETACEOUS										
	0.00061	0.00170	0.00056	0.00071	0.00045	0.00069	0.00045	0.98602	1.52150	
Banachów IG 1	0.00027	0.00400	0.00007	0.00198	0.00004	0.00053	0.00028	0.03946	0.70361	2.27
2354.6 m	0.00050	0.00119	0.00052	0.00044	0.00037	0.00044	0.00044	0.02561	1	
	0.02529	0.49649	0.00348	0.24620	0.00251	0.04516	0.03142	1	4	
	0.00092	0.00450	0.00066	0.00202	0.00052	0.00131	0.00079	0.97019	1.40110	
Cykowo IG 1	0.00250	0.02913	0.00068	0.01421	0.00048	0.00537	0.00271	0.11970	0.62538	16.30
935.8 m	0.00050	0.00119	0.00052	0.00044	0.00037	0.00044	0.00044	0.02248	1	
	0.05468	0.91701	0.01311	0.45520	0.00934	0.12051	0.06389	1	5	
	0.00061	0.00178	0.00056	0.00074	0.00045	0.00068	0.00048	0.98700	1.38530	
Koło IG 3	0.00063	0.00542	0.00020	0.00259	0.00014	0.00123	0.00054	0.05285	0.62945	2.44
1911.6 m	0.00050	0.00119	0.00052	0.00044	0.00037	0.00044	0.00044	0.07499	1	
	0.02207	0.22273	0.00724	0.10864	0.00490	0.04435	0.02124	1	5	
	0.00078	0.00362	0.00060	0.00163	0.00048	0.00102	0.00065	0.97966	1.42980	
Pągów IG 1	0.00222	0.03090	0.00052	0.01520	0.00035	0.00459	0.00246	0.09013	0.65547	19.68
629.3 m	0.00050	0.00119	0.00052	0.00044	0.00037	0.00044	0.00044	0.01536	1	
	0.07706	1.69650	0.01733	0.84271	0.01150	0.18520	0.08737	1	6	
	0.00063	0.00190	0.00057	0.00080	0.00045	0.00072	0.00049	0.98630	1.42540	
Poddębice PIG 2	0.00080	0.00757	0.00024	0.00364	0.00016	0.00159	0.00091	0.05495	0.65621	9.22
2257.6 m	0.00050	0.00119	0.00052	0.00044	0.00037	0.00044	0.00044	0.04599	1	
	0.03058	0.43166	0.00848	0.21237	0.00563	0.06460	0.05402	1	5	

	0.00061	0.00167	0.00057	0.00069	0.00045	0.00068	0.00047	0.98630	1.44850	
Ponętów 2	0.00022	0.00137	0.00009	0.00066	0.00006	0.00046	0.00017	0.04347	0.64991	2.92
1632.6 m	0.00050	0.00119	0.00052	0.00044	0.00037	0.00044	0.00044	0.06345	1	
	0.00780	0.07394	0.00262	0.03621	0.00178	0.01936	0.00734	1	4	
	0.00066	0.00220	0.00057	0.00094	0.00046	0.00077	0.00052	0.98626	1.41290	
Sarnów IG 1	0.00163	0.01731	0.00043	0.00840	0.00029	0.00311	0.00166	0.05726	0.65314	7.88
1741.2 m	0.00050	0.00119	0.00052	0.00044	0.00037	0.00044	0.00044	0.04689	1	
	0.08256	1.19780	0.02579	0.58982	0.01777	0.18905	0.08753	1	5	
	0.00070	0.00286	0.00059	0.00126	0.00047	0.00086	0.00056	0.98342	1.43690	
Strzelno IG 1	0.00200	0.03540	0.00045	0.01752	0.00031	0.00400	0.00204	0.06893	0.66482	7.73
1134.2 m	0.00050	0.00119	0.00052	0.00044	0.00037	0.00044	0.00044	0.01010	1	
	0.09106	2.12970	0.01527	1.06140	0.00987	0.15563	0.08778	1	10	
SANDSTONES OF THE UPPER CRETACEOUS										
	0.00063	0.00174	0.00058	0.00071	0.00046	0.00071	0.00048	0.98614	1.4604	
Koło IG 4	0.00037	0.00215	0.00017	0.00098	0.00012	0.00067	0.00030	0.04050	0.64499	1.22
827.2m	0.00050	0.00119	0.00052	0.00044	0.00037	0.00044	0.00044	0.24736	1	
	0.01519	0.09592	0.00593	0.04383	0.00413	0.02690	0.01222	1	3	
	0.00064	0.00196	0.00057	0.00082	0.00046	0.00071	0.00051	0.98611	1.3742	
Pągów IG 1	0.00072	0.00849	0.00022	0.00415	0.00015	0.00137	0.00071	0.05871	0.60092	7.83
58.3 m	0.00050	0.00119	0.00052	0.00044	0.00037	0.00044	0.00044	0.02060	1	
	0.02546	0.52883	0.00821	0.26267	0.00554	0.05599	0.02428	1	4	
	0.00063	0.00203	0.00057	0.00086	0.00046	0.00070	0.00050	0.98661	1.3908	
Pągów IG 1	0.00077	0.02162	0.00015	0.01077	0.00010	0.00160	0.00088	0.05081	0.60623	3.90
173.8 m	0.00050	0.00119	0.00052	0.00044	0.00037	0.00044	0.00044	0.0069983	1	

	0.05592	2.09980	0.00497	1.04760	0.00337	0.12868	0.07222	1	3	
	0.00071	0.00291	0.00059	0.00128	0.00047	0.00089	0.00058	0.98223	1.4011	
Pągów IG 1	0.00181	0.03060	0.00041	0.01513	0.00028	0.00456	0.00200	0.07606	0.62972	14.14
616.3 m	0.00050	0.00119	0.00052	0.00044	0.00037	0.00044	0.00044	0.01838	1	
	0.08272	1.78530	0.01104	0.88661	0.00754	0.28112	0.09575	1	4	
	mean	standard deviation		minimum	maximum					